VERIFICATION OF KAM THEORY ON EARTH ORBITING SATELLITES

THESIS

Christian L. Bisher, Lieutenant, USN

AFIT/GAE/ENY/10-M03

DEPARTMENT OF THE AIR FORCE
AIR UNIVERSITY

AIR FORCE INSTITUTE OF TECHNOLOGY

Wright-Patterson Air Force Base, Ohio

AFIT/GAE/ENY/10-M03

VERIFICATION OF KAM THEORY ON EARTH ORBITING SATELLITES

THESIS

Presented to the Faculty

Department of Aeronautics and Astronautics

Graduate School of Engineering and Management

Air Force Institute of Technology

Air University

Air Education and Training Command

In Partial Fulfillment of the Requirements for the

Degree of Master of Science in Aeronautical Engineering

Christian L. Bisher, BS

Lieutenant, USN

March 2010

AFIT/GAE/ENY/10-M03

VERIFICATION OF KAM THEORY ON EARTH ORBITING SATELLITES

Christian L. Bisher, BS

Lieutenant, USN

Approved:

William E. Wiesel Jr., PhD (Chairman)	Date
Douglas D. Decker, Lt Col, USAF (Member)	Date
Ronald J. Simmons, Lt Col, USAF (Member)	Date

Abstract

This paper uses KAM torus theory and Simplified General Perturbations 4 (SGP4) orbit prediction techniques compiled by Dr. William Wiesel and compares it to Analytical Graphics® Incorporated (AGI) Satellite Toolkit® (STK) orbit data. The goal of this paper is to verify KAM torus theory can be used to describe and propagate an Earth satellite orbit with similar accuracy to existing general perturbation techniques. Using SGP4 code including only truncated geopotential effects, KAM torus generating code, and other utilities were used to describe a particular satellite orbit as a torus and then propagate the satellite using traditional and KAM torus techniques. These results were compared with similar data generated from initial conditions in STK. Comparisons show orbit prediction for this particular satellite can be made with low kilometer level accuracy. It is claimed with increased mathematical precision and orbital model detail, KAM torus theory applied to orbit prediction techniques can produce more accurate results than currently achievable.

Acknowledgements

I would like to thank my wife for her support and love. Although it was shore duty, the amount of time spent together felt more like a sea tour. With classes during the day and homework or studying during the evenings and weekends, I did not have much free time. You took care of our daughter and went through a difficult pregnancy with our son. You left friends, family, and work in warm and sunny California for cold, new Ohio. All with a smile on your face... at least most of the time. I love you and thank you.

I'd also like to thank Dr. Wiesel for allowing me to take on this task. It was a very challenging and complicated topic, but I enjoyed working on it and hope I helped a little.

Christian L. Bisher

Table of Contents

Page

List of Figures

List of Tables

List of Symbols

Symbol		Page
q	Generalized Coordinates	7
T	Kinetic Energy	7
V	Potential Energy	8
£	Lagrangian	8
$\dot{q}$	Generalized Velocity	8
p	Generalized Momenta	8
$\mathcal{H}$	Hamiltonian	9
μ	Gravitational Parameter	11
$R_\oplus$	Earth's Radius	12
P_n^m	Legendre Polynomials	12
C_{nm}	Geopotential Field Cosine Coefficients	12
S_{nm}	Geopotential Field Sine Coefficients	12
r	Satellite to Center of Earth Radius	12
δ	Geocentric Latitude	12
λ	East Longtiude	12
$\omega_\oplus$	Earth's rotational angular velocity	13
$\mathcal{K}$	New Hamiltonian	16
Q	New Generalized Coordinate	16
P	New Generalized Momenta	16
$\mathcal{H}_0$	Unperturbed Hamiltonian	19
$\mathcal{H}_1$	Lightly Perturbed, Periodic Hamiltonian	19
I	Action Integral Coordinates	19
ϕ	Angle Variable Momenta	19

List of Abbreviations

VERIFICATION OF KAM THEORY ON EARTH ORBITING SATELLITES

I. Introduction

The Air Force's Joint Space Operations Center is tasked with constantly providing United States Strategic Command a space situational awareness picture. All objects orbiting the Earth ten centimeters across or larger are detected, tracked, identified, and cataloged. The sum total of all these objects is a computerized library of over 17,000 man-made objects called the Space Catalog. JSpOC personnel rely on only twenty-nine space surveillance sensors worldwide to accurately maintain position data for all objects in the Space Catalog [3]. The sheer number of items requiring tracking with so few assets shows how daunting a task this can be.

1.1 Motivation

Current general perturbation orbit prediction techniques produce acceptable results for low priority objects. However, there is plenty of room for improvement. Higher priority missions such as manned space walks, collision avoidance, and atmospheric re-entry already require numerical integration for orbit prediction [4]. In either case, as time increases so does location uncertainty. The location uncertainty is an ellipsoid in which the object most likely resides. Location determination techniques produce an estimate of an objects location. Assumptions or errors residing in the technique or equipment used correspond to location errors. In Figure 1.1, the location uncertainty (blue ellipsoid) of a reference satellite is shown growing as time increases. The object must be detected and tracked again before the ellipsoid grows too large and the satellite is lost. If a satellite was lost, meaning its uncertainty ellipsoid had grown too large, resources and time would be required to meticulously scan the entire ellipsoid to reacquire the satellite.

Spacetrack, a phased array radar, is used to track objects in space. A quick search for "Spacetrack problems" on the Internet will show multiple articles detailing new scheduling methods and algorithms to track as many high priority objects as possi-

ble within a given time period. This research is being completed since tracking all objects with the precision desired is becoming impossible [5]. These articles show current space object tracking is already a problem or soon will be.

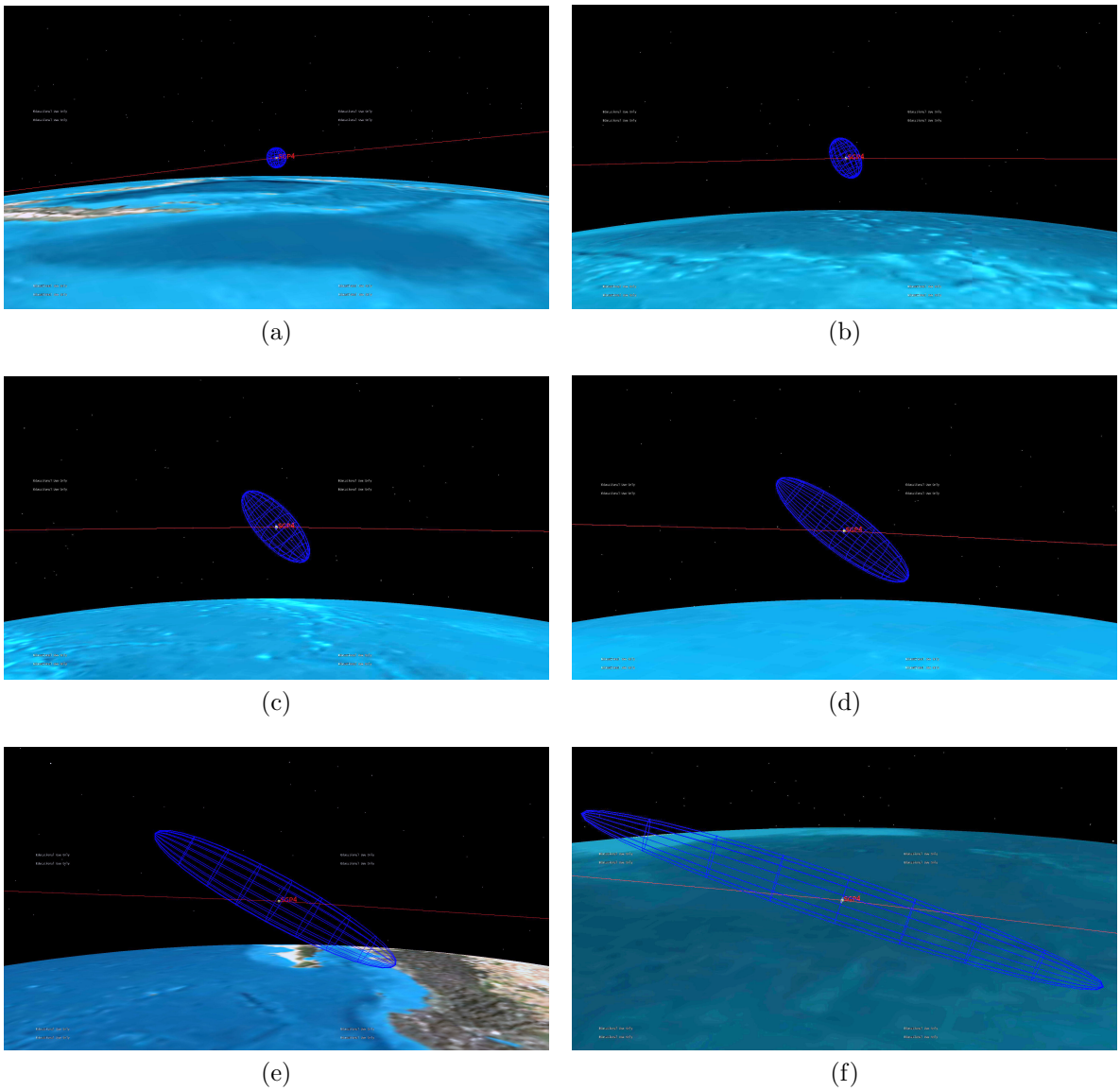

(a) (b) (c) (d) (e) (f)

Figure 1.1: Reference satellite error ellipsoid increasing with time.

On February 10, 2009, a Russian satellite, Cosmos 2251, collided with a U.S. communications satellite, Iridium 33, in orbit. This event produced thousands of pieces of space junk which required tracking. It also increased the chances of one of the other 36 Iridium satellites in similar orbits being hit by 50% [6]. A simulated picture moments

after the collision can be seen in Figure 1.2. Events such as this set to quickly overload current tracking resources.

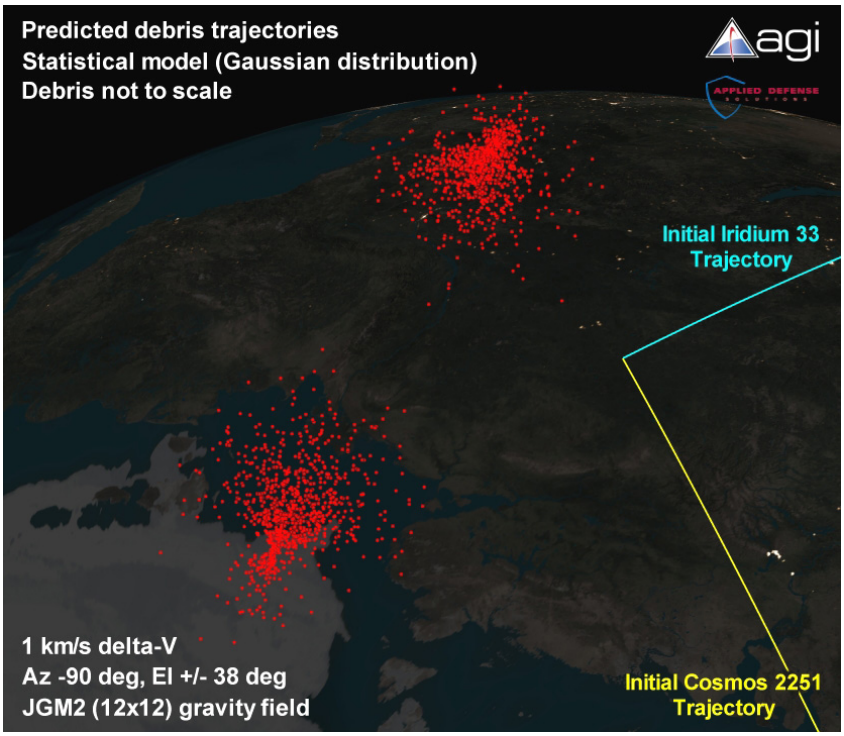

Figure 1.2: A model showing approximate aftermath of the Cosmos / Iridium collision. "Image courtesy of Analytical Graphics, Inc. (www.agi.com)."

1.2 Problem Statement

One option for the overloaded tracking situation is to build more tracking sensors and employ more people to operate and maintain them. This option would cost large amounts of money on both the equipment and manning side. Additional computer resources would also need to be procured. Another option would be to work smarter and find a way to accurately predict these orbiting object's position further out into the future, lessening the frequency with which their tracks need to be updated. Using a theory conceived almost 60 years ago, Dr. William Wiesel at the Air Force Institute of Technology may have found such a method. It utilizes Kolmogorov-Arnol'd-Moser (KAM) theory which is named after the discoverer, A. N. Kolmogorov, and subsequent verifiers, V. I. Arnol'd and J. Moser. Initial work by Dr. Wiesel shows Earth satellite orbits can be described using KAM theory [7]. The current research attempts to validate

the theory against simulated 'real' satellite data produced using Analytical Graphics®, Incorporated (AGI) Satellite Toolkit® (STK).

1.3 Method of Investigation

The object of this paper is to test satellite prediction using KAM theory against current methods. The general perturbations method called Simplified General Perturbations 4 (SGP4) will be used to predict satellite location as the current method. Given the algorithm necessary for SGP4 to produce accurate data for intervals greater than a few days, SGP4 and the KAM theory method cannot be directly compared. To solve this problem STK will be used as an intermediary. STK will be compared to SGP4 to ensure similar or better results are achieved with the more accurate STK numerical integrator. STK orbit data will then be compared to the KAM theory method. If similar results are achieved, then it will have been shown that KAM theory orbit prediction is at least as accurate as the current SGP4. As an initial step it is important to verify KAM theory can be applied to Earth orbiting satellites. Once this is complete more detail can be added to the KAM theory method to produced better results than currently achievable in less time.

Actual Earth satellites will be used, but their location data will be produced from AGI's STK software. Previous investigations by Little [8] used actual satellite location data provided from a satellite team, but problems were encountered when satellite maneuvers were made. Using the STK software, accurate location data can be used while removing any outside influence on the problem, allowing the two methods to be more accurately compared.

1.4 Results

Comparison between KAM torus orbit prediction techniques and STK data as a truth model resulted in position differences under 3.5 kilometers out to 120 days. This research is another source that proves Earth orbiting satellites can be modeled as a torus using KAM theory and propagated accurately. The next step would be to incorporate more detail into the KAM torus model and compare to similar detailed STK data. Upon

successful comparison, the detailed KAM torus model would be compared with an actual satellite and its positional data. Given the accuracy level desired, quadruple precision is most likely required.

II. Background

2.1 Hamiltonian Dynamics

From the publication of Sir Isaac Newton's *Philosophiae Naturalis Principia Mathematica* in 1687 up until the late eighteenth century, Newtonian Mechanics was mechanics [9]. With $F = ma$, forces on single particles, or systems of particles, were used to solve problems of the day. However, Newtonian mechanics had its drawbacks and some problems could not be solved easily. In 1788, Joseph-Louis Lagrange published *Mécanique Analytique* and analytical mechanics was born. In 1834, William Hamilton released two papers on general methods in dynamics in which he applied his principle to the Lagrangian [9]. This was manipulated into the Hamiltonian and Hamiltonian's equations of motion, which described the system [10].

It should be noted that in this paper, systems are assumed to be holonomic, conservative systems. The material in this paper does apply to other systems as well, but this constraint helps lessen the complexity. A few topics must be covered before jumping right into the Hamiltonian, the first being generalized coordinates.

2.1.1 Generalized Coordinates. Most people are familiar with the standard Cartesian coordinate system of x, y, and z. However, there are many other types of coordinate systems: polar, spherical, and cylindrical to mention a few. These coordinate systems help describe the position of an object in a particular frame of reference or space. Generalized coordinates can be thought of as a way of describing a system without being restricted to physical positional coordinates. This idea expanded how a system could be described and allowed problems to be solved in many new ways.

The coordinates of a system can indeed be the x, y, and z position of an object in space, but they could also be the frequencies describing its periodic motion, the coefficients of a Fourier series expansion, a set of angles, or almost anything else. The concept of generalized coordinates allows the coordinates to be almost anything. Most problems can be solved in multiple coordinate systems and using a different system may make a problem much easier to solve. Changing from physical to non-physical coordiantes could give new insight to an existing problem or make its solution easier. Generalized

coordinates, q, are most commonly referred to as,

$$\boldsymbol{q} = (q_1, q_2, q_3, \ldots, q_n), \tag{2.1}$$

and for the problem presented here are,

$$\boldsymbol{q} = \left\{ \begin{array}{c} x \\ y \\ z \end{array} \right\}. \tag{2.2}$$

The number of coordinates helps determine the dimensionality of a problem.

2.1.2 Dimensionality. Another concept that must be grasped is dimensionality. We all live, work, and are most familiar in three-dimensional space. However, mathematical problems are not restricted to three dimensions. A simple pendulum could have three coordinates while a more complicated problem could have six coordinates or more. Although a six dimensional object cannot be visualized in three dimensional space, the mathematics behind the problem work just fine. Later in this paper when six dimensional objects are discussed, think of a three dimensional object for visualization purposes, but realize the actual dimensionality is greater.

2.1.3 The Lagrangian. As mentioned earlier, Lagrange initiated what is now know as analytical mechanics. However, he relied on Jean le Rond d'Alembert's 1743 work, *"Traité de dynamique"*, where d'Alembert revealed his principle,

$$\sum_{k=1}^{N} (\boldsymbol{F}_k - \dot{\boldsymbol{p}}_k) \cdot \delta \boldsymbol{r}_k = 0. \tag{2.3}$$

With this principle, a dynamic problem is treated as a static one. The total virtual work done on a system by infinitesimal virtual displacements is equal to zero [10].

Using d'Alembert's principle and work by Euler, Lagrange began thinking of the system as a whole and the total energy of the system, instead of individual particles. Energy comes in two forms, potential and kinetic. Kinetic energy (T) is the energy of a

system based on its motion and is given by,

$$T = \frac{1}{2}mv^2. \tag{2.4}$$

While potential energy (V) is the energy stored within the system. For systems near the surface of the Earth, the potential energy will be based on position and can be given by,

$$V = mgh. \tag{2.5}$$

However, in dealing with celestial bodies and their gravitational fields a different approach must be used. For the moment the above representation is sufficient, but a more accurate model will be discussed in Section 2.2.1.

A cornerstone to analytical dynamics is a mathematical expression called the Lagrangian ($\pounds$), which is the difference between the kinetic and potential energy of a system,

$$\pounds = T - V. \tag{2.6}$$

The Lagrangian is called a descriptive function for a system, because it contains all the information necessary to produce the equations of motion for the system. However, the Lagrangian produces n second-order differential equations, where n is the number of coordinates for the system,

$$\frac{d}{dt}\left(\frac{\partial \pounds}{\partial \dot{q_n}}\right) - \frac{\partial \pounds}{\partial q_n} = 0. \tag{2.7}$$

While second-order differential equations can be solved, first-order differential equations would be easier to solve.

The time derivatives of generalized coordinates are generalized velocities, $\dot{q}$. The derivative of the Lagrangian with respect to the generalized velocities are the generalized momenta,

$$p_n = \frac{\partial \pounds}{\partial \dot{q_n}}. \tag{2.8}$$

Generalized coordinates and generalized momenta come in pairs, thus they are normally referred to as conjugates of each other. If a generalized coordinate or momenta does not

appear in the Lagrangian, then its conjugate is cyclic, or ignorable, and is constant. If a generalized coordinate or momenta is constant, a conservation law is within the problem and much can usually be determined about the system without ever having to solve the problem [10].

2.1.4 Hamilton's Principle. William Rowan Hamilton began applying variational calculus to previous work in the emerging field of analytical mechanics. He looked at the entire dynamical system between two points in time, t_1 and t_2 [10]. With varia-

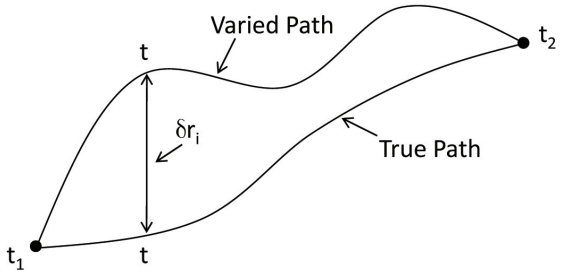

Figure 2.1: Hamilton's Principle

tional calculus, the path between these two points can vary as long as the endpoints stay fixed. Integrating over this distance produces a scalar integral which is independent of the coordinates of the Lagrangian [10],

$$\delta I = \delta \int_{t_1}^{t_2} \pounds dt = 0. \tag{2.9}$$

Hamilton's principle is essentially an integrated form of d'Alembert's Principle. Instead of using d'Alembert's Principle to derive Lagrange's equations of motion, Hamilton's Principle offered an easier way which was not dependent on physical coordinates [10].

2.1.5 Hamilton's Equation. While Lagrange's equations of motion are a set of n second-order differential equations, Hamilton's equations of motion are a set of $2n$ first-order differential equations [10]. The Hamiltonian, $\mathcal{H}$, can initially be defined as,

$$\mathcal{H} = \sum_{k=1}^{n} \frac{\partial \pounds}{\partial \dot{q}_k} \dot{q}_k - \pounds. \tag{2.10}$$

To get first-order differential equations and the Hamiltonian in the correct form, the conjugate momenta, Equation 2.8, must be substituted into Equation 2.10 [10],

$$\mathcal{H} = \sum_{k=1}^{n} p_k \dot{q}_k - \pounds. \tag{2.11}$$

The Hamiltonian equations of motion are then the partial derivatives of the Hamiltonian with respect to the generalized momenta and negative generalized coordinates [10],

$$\dot{q_k} = \frac{\partial \mathcal{H}}{\partial p_k}, \tag{2.12}$$

$$\dot{p_k} = -\frac{\partial \mathcal{H}}{\partial q_k}. \tag{2.13}$$

Finally a set of $2n$ first-order differential equations, also known as Hamilton canonical equations, are ready to be solved. The combination of variables q_k and p_k that solve the above equations can be plotted, and the trajectory of these points through time shows the motion of the system. These points can then be plotted in phase space [10].

2.1.6 Phase Space. For mathematical problems in grade school, Euclidean space was most likely used because its properties were well suited for geometrically showing solutions to the mathematics being worked on at the time. When dealing with Hamiltonian mechanics, phase space is used. The spot in phase space where the generalized coordinates and conjugate momenta produce a solution to the Hamilton canonical equations a point is produced. The combination of all these points represents the motion of the system in phase space. While Euclidean space has three dimensions when n equals three, phase space would have $2n$ dimensions, or six. Since graphing in the six-dimensional space is impossible, phase space plots usually include only two or three of the variables at a time [10].

2.2 Earth Orbiting Satellite

2.2.1 The Geopotential. The geopotential for a given celestial object is its gravitational field. This gravitational field exerts a force on objects based on their

distance from the celestial body and the mass of the celestial body. An example of the two body problem is a small object orbiting around a larger object. The small object, a

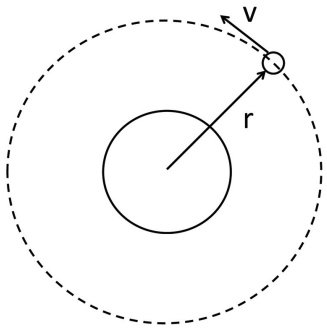

Figure 2.2: The Two Body Problem

satellite for example, is a distance r from the center of the larger object, the Earth for example. The satellite is traveling with a velocity, v, and should continue in a straight line off the page. However, the mass of the Earth creates a gravitational field in which an attractive force is exerted upon the satellite. This attractive force and the velocity of the satellite form an equilibrium that allows the satellite to stay in an orbit around the Earth. The attractive force the Earth exerts on the satellite is the potential energy and for the two body problem is given by,

$$V = \frac{\mu}{r}, \tag{2.14}$$

where r is the distance from the satellite to the center of the Earth and μ is a gravitational parameter for the Earth, which is based on the mass and gravitational constant of the Earth [10].

The two body gravity model provides decent estimates for simplified problems. However, more complicated problems require a better estimate for the geopotential. In this research the geopotential will be estimated using the following equation,

$$V = -\frac{\mu}{r}\sum_{n=1}^{\infty}\sum_{m=1}^{n}(\frac{r}{R_{\oplus}})^{-n}P_n^m(\sin\delta)(C_{nm}\cos m\lambda + S_{nm}\sin m\lambda), \tag{2.15}$$

where the Earth's gravitational parameter is again μ and the Earth's equatorial radius is $R_\oplus$. The Legendre polynomials, P_n^m, and the field coefficients, C_{nm} and S_{nm}) are used to help describe the geopotential more precisely anywhere around the Earth's sphere. The radius to the satellite from the center of the Earth (r), the geocentric latitude (δ), and the east longitude (λ) are found from [7],

$$r = \sqrt{x^2 + y^2 + z^2}, \tag{2.16}$$

$$\sin\delta = \frac{z}{\sqrt{x^2 + y^2}}, \tag{2.17}$$

$$\tan\lambda = \frac{y}{x}. \tag{2.18}$$

The geocentric latitude is the angle between the equatorial plane and a line from the center of the Earth to a point on the surface. This value is less than the geodetic latitude more commonly used which is the angle between the equatorial plane and a line normal to the Earth's surface.

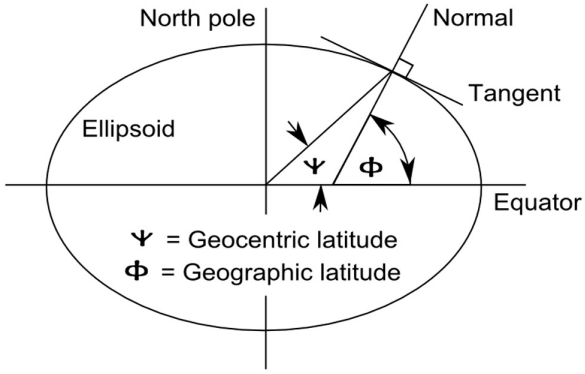

Figure 2.3: Geocentric and Geographic Latitudes [1]

The gravity model used by Dr. Wiesel's SGP4 is EGM96, or the Earth Gravity Model completed in 1996. For Equation 2.15, terms to degree (m=20) and order (n=20) are used. Although sufficient for application in this research, the EGM96 model does go up to order and degree 360. An example of the variation in geopotential can be seen in Figure 2.4 [2].

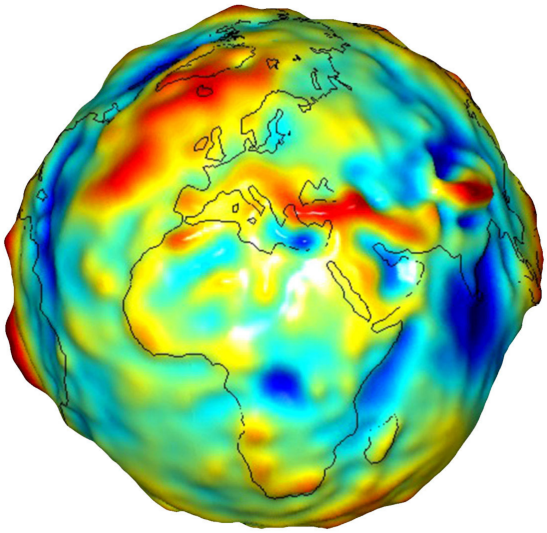

Figure 2.4: GRACE Gravity Model, Europe and Africa [2]

2.2.2 Hamiltonian. For an Earth satellite Hamiltonian, an Earth-Centered, Earth-Fixed (ECEF) reference frame will be used. Earth-Centered means the center of the Earth is at the origin of the reference frame, and Earth-Fixed means the Earth appears stationary with respect to the reference frame. In actuality the Earth is still revolving, however, since the reference frame is revolving with the Earth it looks fixed. The Hamiltonian can be written as [7],

$$\mathcal{H} = \frac{1}{2}(p_x^2 + p_y^2 + p_z^2) + \omega_\oplus(yp_x - xp_y) \\ - \frac{\mu}{r}\sum_{n=1}^{\infty}\sum_{m=1}^{n}\left(\frac{r}{R_\oplus}\right)^{-n} P_n^m(\sin\delta)(C_{nm}\cos m\lambda + S_{nm}\sin m\lambda). \tag{2.19}$$

The Earth's rotational angular velocity is given by $\omega_\oplus$. The entire last term of Equation 2.19 is the Earth's geopotential as described earlier. The generalized coordinates and momenta are then,

$$\boldsymbol{q} = \begin{Bmatrix} x \\ y \\ z \end{Bmatrix}, \tag{2.20}$$

$$\boldsymbol{p} = \begin{Bmatrix} p_x \\ p_y \\ p_z \end{Bmatrix}. \tag{2.21}$$

As was the Lagrangian, the Hamiltonian is also a descriptive function in that the equations of motion for the system can be obtained from it. These equations of motion are called Hamilton canonical equations [10],

$$\dot{\boldsymbol{q}} = \left\{ \begin{array}{c} -\omega_{\oplus} p_y - \frac{\partial V}{\partial x} \\ \omega_{\oplus} p_x - \frac{\partial V}{\partial y} \\ -\frac{\partial V}{\partial z} \end{array} \right\}, \quad (2.22) \qquad \dot{\boldsymbol{p}} = \left\{ \begin{array}{c} p_x + \omega_{\oplus} y \\ p_y - \omega_{\oplus} x \\ p_z \end{array} \right\}. \quad (2.23)$$

A complete derivation of the above Hamiltonian and canonical equations can be found in Appendix B.

2.2.3 Numerical Integration. In this research, the SGP4 propagator will be compared to a numerical integration for a reference satellite's orbit. To do this, the above Hamiltonian will be numerically integrated using a Hamming fourth-order predictor-corrector algorithm [7]. The following numerical integrator description was referenced from Dr. Wiesel's Hamming Fortran program. First, the initial conditions of the orbit are assigned to a state vector. These initial conditions are the generalized coordinates and momenta at the start of the integration when time is equal to zero,

$$\boldsymbol{x} = \left\{ \begin{array}{c} \boldsymbol{q} \\ \boldsymbol{p} \end{array} \right\} = \left\{ \begin{array}{c} x \\ y \\ z \\ \dot{x} \\ \dot{y} \\ \dot{z} \end{array} \right\}. \quad (2.24)$$

Second, the derivative of the state vector is taken and the Hamilton canonical equations are substituted in for $\dot{\boldsymbol{q}}$ and $\dot{\boldsymbol{p}}$,

$$\dot{\boldsymbol{x}} = \left\{ \begin{array}{c} \dot{\boldsymbol{q}} \\ \dot{\boldsymbol{p}} \end{array} \right\} = \left\{ \begin{array}{c} \frac{\partial \mathcal{H}}{\partial p_k} \\ -\frac{\partial \mathcal{H}}{\partial q_k} \end{array} \right\} = \left\{ \begin{array}{c} -\omega_{\oplus} p_y - \frac{\partial V}{\partial x} \\ \omega_{\oplus} p_x - \frac{\partial V}{\partial y} \\ -\frac{\partial V}{\partial z} \\ p_x + \omega_{\oplus} y \\ p_y - \omega_{\oplus} x \\ p_z \end{array} \right\}. \tag{2.25}$$

Next, the total time of the integration is divided by the number of steps taken during the integration to get an incremental time step (dt). Finally, the future position is the old position plus the change in position multiplied by the time step,

$$\boldsymbol{x_{i+1}} = \boldsymbol{x_i} + \dot{\boldsymbol{x}}_{\boldsymbol{i}} dt. \tag{2.26}$$

Numerical integration, though accurate, is very computationally expensive and thus requires large amounts of computer resources. All publicly available orbit data from the DOD Space-Track website is propagated with SGP4. However, numerical integration may be used within the Air Force for high priority objects, collision avoidance situations, and the two weeks before large objects re-enter Earth's atmosphere [4].

2.2.4 SGP4. Simplified General Perturbation 4 (SGP4) is the current orbit propagator employed by the United States Air Force. It was developed in the 1960's, went operational in the 1970's, and has been updated many times during its history [11]. In 1988, North American Aerospace Defense Command (NORAD) decided to release the SGP4 code giving end users of NORAD two-line element (TLE) sets the ability to propagate Earth orbiting objects [12]. Since that time, both military and civilian users updated their copy of SGP4 to fit a specific use. This created many working versions of the code. In 2006, a group of four individuals consolidated these working versions into a standard version of SGP4 that hopefully matched the Department of Defense (DoD)

version [11]. The Air Force has not released information on object orbit propagation since 1988, so it is impossible to know for sure what is being used.

SGP4 treats orbiting objects as either near-Earth or deep-space, with the boundary at an orbital period of 225 minutes. Earth's geopotential, air drag, solar pressure, and lunar effects are all accounted for within SGP4. However, the 1980 version of SGP4 used in this research only accounts for the Earth's geopotential to order and degree 20 [11].

2.3 Transformation Theory

2.3.1 Generating Functions. Hamiltonian's have a property in that a coordinate transformation can be made to a different Hamiltonian with different coordinates and momenta while still describing the same system. These transformations provide an opportunity to look at a single problem multiple ways. Quite frequently, a different Hamiltonian will have coordinates and momenta such that the problem is solvable or simplified [13]. A similar idea is carried out when a person in a room is identified by saying "look at two o'clock" instead of saying "look 6 feet east and 8 foot north". Both commands point in relatively the same direction, but one gets there faster and easier.

It is possible to switch to a new Hamiltonian, but how and which one? In letters from 1836 and 1837, Carl Gustav Jacobi answered this question with the Hamilton-Jacobi transformation theory [14]. He was able to learn, use, and improve upon the ideas Hamilton had only released a few years earlier.

There should be some function, F, that will take the old coordinates and momenta and transform them into the new coordinates and momenta. At this point neither the function, the new coordinates, or the new momenta are known, but the statement is still accurate. Therefore, the new coordinates, Q, and momenta, P, should be functions of the old coordinates, q, and momenta, p, and the new Hamiltonian, $\mathcal{K}$, should be a function of the new coordinates and momenta [13],

$$Q = Q(q_n, p_n, t), \tag{2.27}$$

$$P = P(q_n, p_n, t), \tag{2.28}$$

$$\mathcal{K} = \mathcal{K}(Q, P, t). \tag{2.29}$$

With one set of old and one set of new coordinates and momenta, there are four possible combinations. These four combinations translate to four different functions that transform from the old to the new Hamiltonian. Each function has one old and one new coordinate and momenta, and with this information the remaining two coordinates and momenta can be determined [13].

For this problem, the F_2 generating function will be used which also happens to be the most frequently used function. The properties of the F_2 generating function are listed below [15].

$$F_2 = F_2(q_n, P_n, t), \tag{2.30}$$

$$p_i = \frac{\partial F_2}{\partial q_i}, \tag{2.31}$$

$$Q_i = \frac{\partial F_2}{\partial P_i}. \tag{2.32}$$

By changing the coordinate and momenta combinations in Equation 2.30, the other three functions and relations can be identified.

At this point, the author will skip forward to the relationship between the old and new Hamiltonians. If more information is desired on generating functions or the transformation itself, please see reference [13], pages 43-58. Essentially, the derivative of the F_2 function with respect to time is broken down into a sum of its partial derivatives with respect to the old coordinates, separated, and substituted in for the new momenta which creates the generating function. This also explains why the partial of the F_2 with respect to time remains [13].

2.3.2 Hamilton-Jacobi Equation. There is now enough information to form a relationship between the new and old Hamiltonians [13],

$$\mathcal{K}(Q_k, P_k) = \mathcal{H}(q_k, p_k) + \frac{\partial F}{\partial t}. \tag{2.33}$$

Recall that when a coordinate or momenta is missing from the Lagrangian or Hamiltonian, the conjugate momenta or coordinate is a constant. Therefore, if the new coordinate and momenta do not appear in the new Hamiltonian, then the new Hamilton canonical equations would be equal to zero [13].

$$\dot{Q}_k = \frac{\partial \mathcal{K}}{\partial P_k}, \tag{2.34}$$

$$\dot{P}_k = -\frac{\partial \mathcal{K}}{\partial Q_k}. \tag{2.35}$$

If the Hamilton canonical equations are zero and the new coordinates and momenta are constant, the new Hamiltonian must equal zero. This changes Equation 2.33 into the Hamilton-Jacobi equation [13],

$$\mathcal{H}(q_k, p_k) + \frac{\partial F}{\partial t} = 0. \tag{2.36}$$

This process exentially seeks out a generating function such that the new coordinates and momenta are integrals of the motion and the new Hamiltonian is zero. As can be expected, this transformation greatly simplifies the problem.

2.4 KAM Theory

KAM theory's beginnings were initially proposed by A.N. Kolmogorov in his 1954 paper, "On conservation of conditionally periodic motions for a small change in Hamilton's function." In the 1960's, J. Moser and V.I. Arnol'd proved the theory after releasing multiple papers [9]. Relatively speaking, this powerful theory has gone unused.

For a completely solvable, or integrable, Hamiltonian, all solutions lie on a n-dimensional torus in $2n$-dimensional phase space, where n is the number of coordinates. KAM theory simply states, lightly perturbed Hamiltonian systems will have most of their solutions still lying on the surface of an invariant torus given the perturbation is small enough [16],[17],

$$\mathcal{H} = \mathcal{H}_0(I) + \epsilon \mathcal{H}_1(I, \phi), \;\; \epsilon \ll 1. \tag{2.37}$$

In the above equation, $\mathcal{H}_0$ is the Hamiltonian of the unperturbed problem, $\mathcal{H}_1$ is the perturbed, periodic Hamiltonian, and ϵ indicates the perturbations are very small. The above Hamiltonians for the KAM torus are in action-angle variable form, meaning action integral variables, I, are the coordinates, q's, and angle variables, ϕ, are the conjugate momenta, p's. Since the coordinates and momenta are different than our current Earth satellite Hamiltonian, Equation 2.19, a transformation must be used. The process discussed in Section 2.3 concerning generating functions and the Hamilton-Jacobi equation will be used and discussed more in the following section. Notice in Equation 2.37 that the unperturbed system, $\mathcal{H}_0(\mathrm{I})$, is missing the angle variable momenta, ϕ. From Equation 2.12, this means the rate at which the coordinate action integral variable, I, changes is zero, so the action inegral variable is a constant.

Invariant, mentioned above, means once a trajectory in phase space is on an invariant torus it will remain on the torus. As an example, think of a rolling coin. If a coin is rolled on a flat surface there is no telling which direction it will go or which side it will fall onto. This is non-invariant. Now, think of the spiraling coin funnels found in malls and museums. Once the coin is release, barring some outside force such as a child picking the coin up, the coin will continue to roll around in circles and eventually fall down the whole. There is no stopping it and this is invariant. The only difference is the coin eventually stops, but the satellite motion on the KAM torus is periodic so it will continue repeating forever. If an Earth satellite is to lie on a KAM torus, it will do so in phase space and it will be a lightly perturbed invariant torus [7].

2.4.1 Transformation. Discuss here after talking with Wiesel

Earlier, transformation theory and the Hamiltonian-Jacobi equation were discussed. Equation 2.19 is the Hamiltonian for an Earth orbiting satellite with coordinates x, y, and z. The KAM theory Hamiltonian, Equation 2.37, is in action and angle variables. To see if Earth orbits can be described using KAM tori, it is necessary to transform the Earth satellite Hamiltonian, Equation 2.19, into the form of the KAM theory Hamiltonian, Equation 2.37. This can be done using the Hamilton-Jacobi equation, 2.36, and

methods discussed in Section 2.3 on transformation theory. Dr. Wiesel has shown this process in reference [16].

2.4.2 KAM Torus Orbital Coordinates. Dr. Wiesel applied a Fast Fourier Transform (FFT) algorithm to a one year numerical integration of the reference satellite. The algorithm was able to separate the periodic behavior of the orbit into three base frequencies. Dr. Wiesel shows in [16] that these three frequencies used to describe the KAM torus can be linked to three classical Delaunay orbital elements. The largest of these three frequencies is the 'mean' mean anomaly, M. The second frequency is the longitude of the mean node, Ω. The smallest frequency is the mean argument of perigee, ω. These three angles, with the use of Hamilton-Jacobi theory, will be transformed from the x, y, z positional coordinates of the original Hamiltonian [7] to the coordinates of the new KAM Hamiltonian.

2.4.3 Phase Space KAM Torus. In phase space, the three fundamental frequencies listed above creates a torus of a particular size and shape within $2n$-dimensional phase space that describes the satellite's orbit. The torus is described with a Fourier series including these frequencies. Also, the coordinates and momenta are grouped together into one state vector. During the numerical integration of the satellites orbit, the rate of change of the state vector is found. Using a least squares fitting algorithm, the state vector and its rate of change can be made to fit a Fourier series torus that includes the three fundamental frequencies describing the orbit. Once converged, this gives all the coefficients necessary to uniquely describe the satellite as a Fourier series, which in turn produces a torus in $2n$-dimensional phase space [7].

III. Methodology

This section lays out the processes taken during the course of this research. Since the research was computer simulation, computer and software setup will be discussed first. Any assumptions made during this research will then be listed. Finally, the programing and testing process will be discussed for SGP4, STK, and KAM torus orbit propagation techniques.

3.1 Computer Software

3.1.1 Fortran Programming. The author performed all programming within the Microsoft® Visual Studio® 2008 program development environment on a Windows Vista® 64-bit computer. The compiler was Intel® Visual Fortran Compiler Professional Edition for Windows®, version 11.1.046. Both software suites were used with educational licenses. Almost all Fortran code was previously written and provided to the author by Dr. Wiesel. Code was updated to Fortran 95/2003 wherever possible and edited to run within the Microsoft® Visual Studio® (MVS) environment. Double precision was chosen for all real variables with a user defined length of 15 digits. This helps ensure maximum portability and consistency on different computer systems and allows for future precision changes from one location. The 'IMPLICT NONE' command was always used to minimize possible variable errors.

3.1.2 Commercial Orbit Prediction. In order to help validate previous results, it was necessary to compare to an outside source. Analytical Graphics® (AGI) Satellite Toolkit® (STK) was easily accessible with a free educational license and was recommend by Dr. Wiesel. The author used STK Version 9.0.1, which has multiple propagators that will determine a satellite's position in time. The author choose the High Precision Orbit Propagator (HPOP) due to its ease of use and detailed capabilities far exceeding necessary requirements. The HPOP propagator is a numerical integrator utilizing the differential equations of motion for the satellite initially generated from ephemeris data, as stated in the STK help files. For those unfamiliar, ephemeris data includes position and velocity of a satellite for a given time period. STK allows the user to import a specific satellite file, choose the date and time, and ephemeris data is automatically generated

via an AGI server connection. Almost any force or perturbation can be modeled with the HPOP propagator in great detail.

3.1.3 Plotting. All plotting was completed using the Windows® version of Gnuplot©, Version 4.2.6. The software is free and relatively easy to use for simple graphs. However, the program has many advanced features allowing for very detailed and specific plots. Dr. Wiesel uses Gnuplot and example scripts were easily edited by the author.

3.2 Assumptions

Given the academic nature and initial testing of this theory, certain effects and details have not been accounted for that normally would for a developed technique used by NASA on an actual satellite. The geopotential, Equation 2.15, discussed in Section 2.2.1 is used to calculate the Earth's gravitational force on the satellite as it orbits the Earth. For this research, order and degree truncated to 20 was decided sufficient.

Air drag, ocean tides, lunar and solar gravitational effects, and other third body effects have all been assumed small enough when compared to Earth's gravity to be neglected. If these smaller terms had been accounted for then a more detailed geopotential model, higher order and degree for Equation 2.15, would have been used.

While actual satellite mission orbit prediction would use most if not all the above effects, the mission of this research to show KAM theory can be applied to Earth satellites for orbit prediction can reliably succeed without these effects.

3.3 Reference Satellite

Continuing with Dr. Wiesel's work, the reference satellite for this research will be the same. This will allow for continuity between papers and with future research. The reference satellite's initial conditions are listed in Table 3.1, orbital elements are listed in Table 3.2, and a picture of the orbit is in Figure 3.1.

3.4 SGP4 Verification

Table 3.1: Reference Satellite Initial Conditions

	x	y	z
Position (km)	-4412.83115168178	4676.00408732872	-2910.15168627727
Velocity (km/sec)	-4.42110219123704	-5.02218008450107	-2.27614671171868

Table 3.2: Reference Satellite Orbital Elements

Semi-major Axis	Eccentricity	Inclination	Right Ascension Ascending Node	Argument of Perigee	Mean Anomaly
a	e	i	Ω	ω	M
7,049.5 km	0.05	30.0°	261.72°	141.41°	88.42°

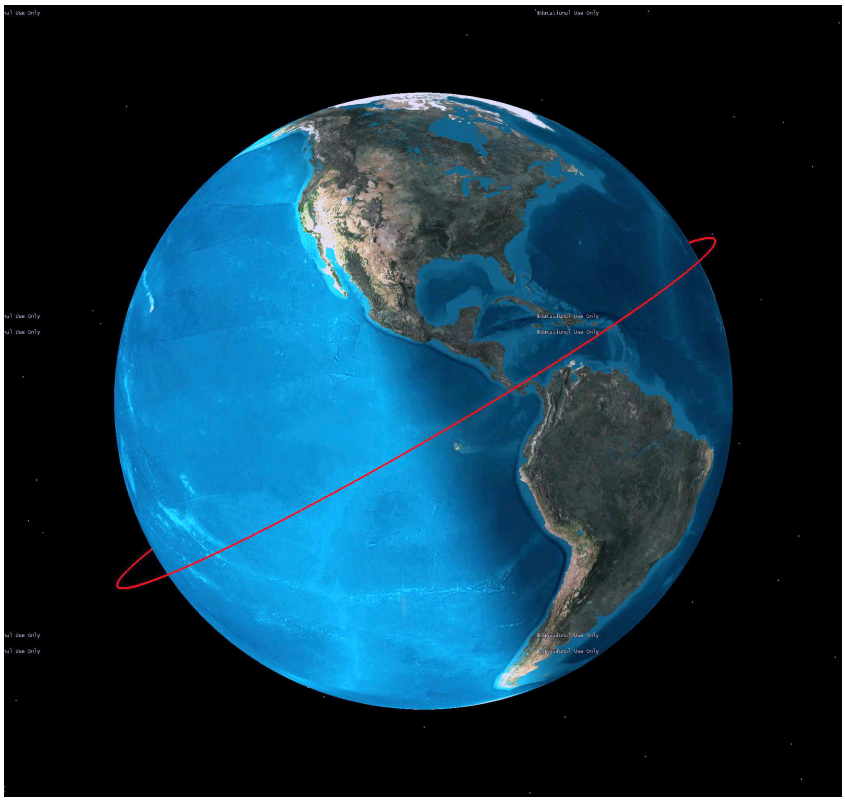

Figure 3.1: Reference Satellite Orbit from STK.

3.4.1 Test Case. The version of SGP4 used is in this research is different from the original 1980 version of SGP4 released by Hoots and Roehrich in [12]. As stated earlier, the author was given Dr. Wiesel's existing Fortran code. The first step was to make sure it would run properly on the author's computer and produce correct results. Starting with the SGP4 program, a test satellite was both numerically integrated using a Hamming fourth-order predictor-corrector algorithm and propagated with SGP4. The

differences in x, y, z position between the numerical integrator and SGP4 results are called the residuals. These residuals are then plotted both individually and together as a total magnitude.

3.4.2 Reference Satellite. For comparison later in this paper, the above process was also completed for the reference satellite discussed above. Throughout this research the reference satellite was used to help ensure proper program operation and for result comparison with other satellites that were used.

3.5 Comparing SGP4 and STK Propagators

Next, the SGP4 satellite propagator was compared to STK's HPOP propagator. The satellites tested were randomly chosen from all orbiting satellites with only two requirements. The first being a relatively equal spacing of satellites in the low Earth orbit (LEO) region. Second, within the LEO group a few satellites had to be very close to each other to compare results. Satellites from medium Earth orbit (MEO) and high Earth orbit (HEO) were not included in this test since the deep-space section of the SGP4 code was not included in the version used in this research. The satellites chosen are listed in the following table with data taken from STK at the initial time prior to propagating. The satellites used in the SGP4 versus STK comparison can be seen in

Table 3.3: STK Satellite Orbital Data & Elements

Satellite	Altitude (km)	Semi-Major Axis (km)	Eccentricity	Inclination (degrees)	Period (mins)
Grace 1	467.94	6839.52	0.00125	88.99°	93.82
Grace 2	468.23	6838.84	0.00133	88.99°	93.81
Swift	584.6	6972.19	0.00196	20.53°	96.56
Reference Satellite	679.28	7049.5	0.05	29.96°	98.17

Figure 3.2.

Each satellite had position and velocity information created with HPOP which was read into the SGP4 and STK Fortran program. The SGP4 propagator used the first line of each satellite's inertial data as the initial conditions and proceeded from there. All tested satellites were initiated with the same start date and time. Satellites were

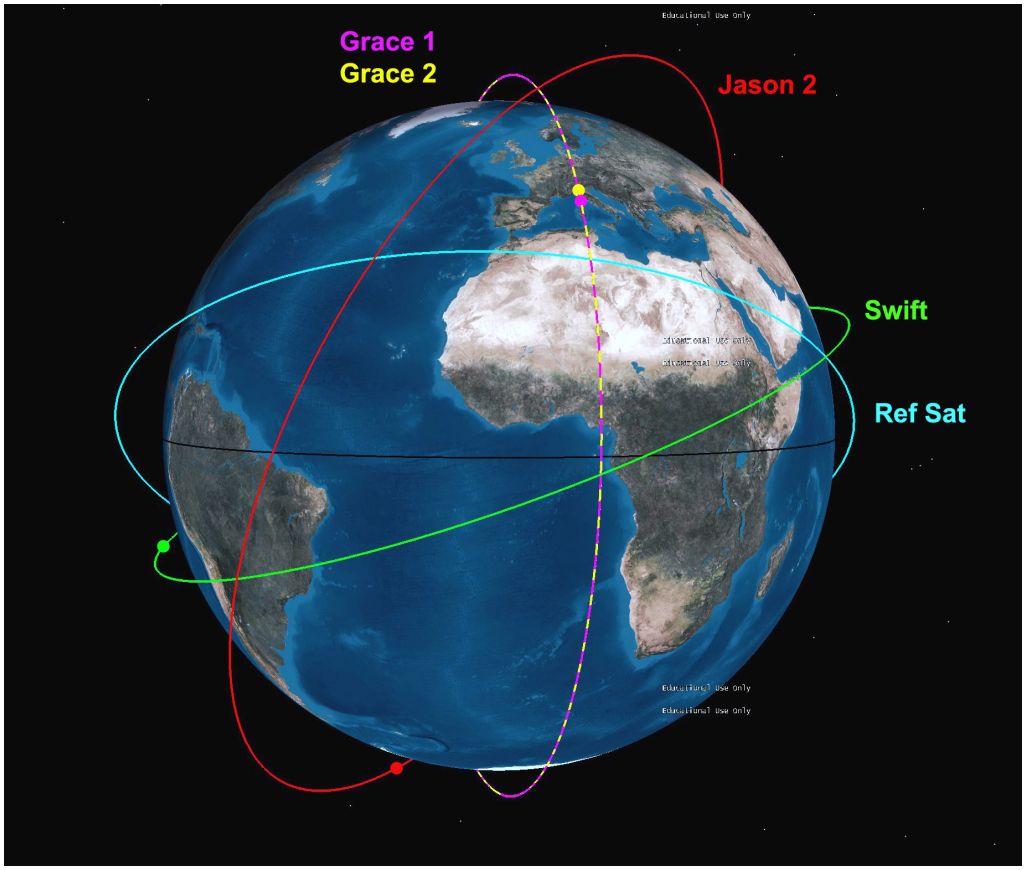

Figure 3.2: Satellites used in SGP4 / STK comparison.

propagated out in increments of 10, 15, 30 and 60 days. The residuals, the difference in location between the two propagators, were calculated at each time step. Each satellite that completed the program and showed residuals of tens of meters or less would then be run with the next higher propagation time step.

3.6 Torus Frequencies

An Earth satellite orbit can be approximated as a KAM torus [7]. The primary purpose of this research is to verify this statement against simulated STK orbit data. Dr. Wiesel numerically integrated a reference satellite for one year, with x, y, z position data stored in a file for each time step. Reference satellite characteristics were discussed in Section 3.3, and the process for finding the three torus frequencies was discussed in Section 2.4.2.

A program written by Dr. Wiesel called 'PeakEater' takes an orbit file with position and time data and produces a file describing a torus. The torus is created using a Fourier series,

$$\boldsymbol{r} = \sum_{\boldsymbol{j}=1}^{n} \boldsymbol{C_j} \cos(\boldsymbol{j} \cdot \boldsymbol{Q}) + \boldsymbol{S_j} \sin(\boldsymbol{j} \cdot \boldsymbol{Q}), \tag{3.1}$$

where $\boldsymbol{C_j}$ and $\boldsymbol{S_j}$ are the Fourier series coefficient vectors, the $\boldsymbol{Q}$ vectors is the three torus frequencies multiplied by time ($\boldsymbol{Q}_i = \boldsymbol{\omega}_i t + \boldsymbol{Q_{0i}}$), and $\boldsymbol{j}$ is an indice vector indicating each torus frequency has its own set of Fourier series coefficients. Remember, the torus has n-dimensions in $2n$-dimensional phase space.

Once the location on a torus is found, that point linearly drifts with time,

$$\boldsymbol{Q} = \left\{ \begin{array}{l} \omega_1 t + Q_{01} \\ \omega_2 t + Q_{02} \\ \omega_3 t + Q_{03} \end{array} \right\}. \tag{3.2}$$

This linear drift around the torus in phase space is the satellite propagating around the orbit in real space.

Using the reference satellite's initial conditions, STK produced a 120 day orbit propagation with HPOP. A program from Dr. Wiesel called 'Coordinate Residuals' compared the STK orbit to the KAM torus Fourier series. Once the location of the STK orbit is found on the torus, the orbit is propagated forward using the time. The location on the torus is then converted back into positional coordinates and these are compared to the STK position to again produce residuals. These residuals are again plotted as individual coordinate residuals and as a residual magnitude.

IV. Results and Discussion

In this section the results will be presented and discussed. As a reminder, coordinate residuals are the differences between each coordinate (x, y, z) for the two methods being compared. Residual magnitude is the magnitude of the residual coordinates for the two methods being compared.

4.1 SGP4 Verification

4.1.1 Test Case. The first step was to ensure all code from Dr. Wiesel was implemented correctly. After running the test case, output plots of coordinate residuals and residual magnitude of all three coordinates were compared. The initial plots using SGP4 matched Dr. Wiesel's and thus confirmed the initial SGP4 propagator and numerical integrators were working. Figure 4.1 shows the x, y, and z residuals between the numerical integration and the SGP4 propagator stayed under 1.2 kilometer for the first 6 days, while Figure 4.2 shows the magnitude of the residual error remained under 1.25 kilometers over the 6 day period.

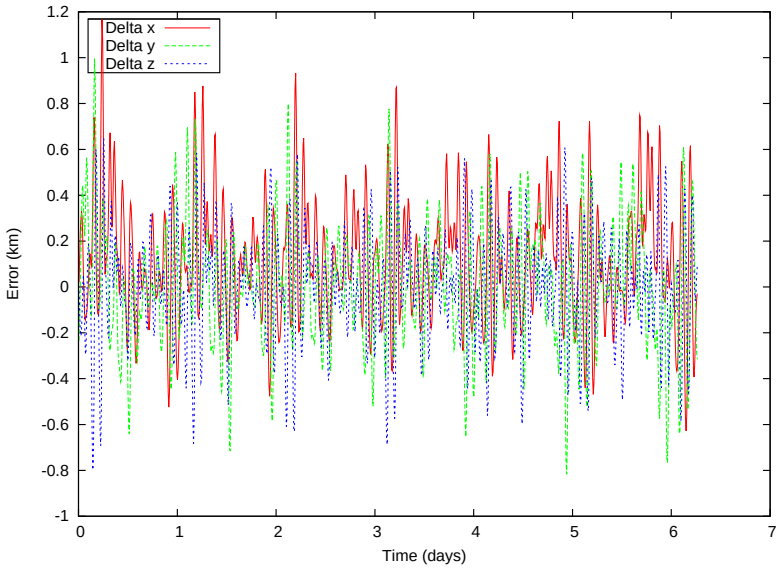

Figure 4.1: SGP4 verification showing coordinate residuals for test case.

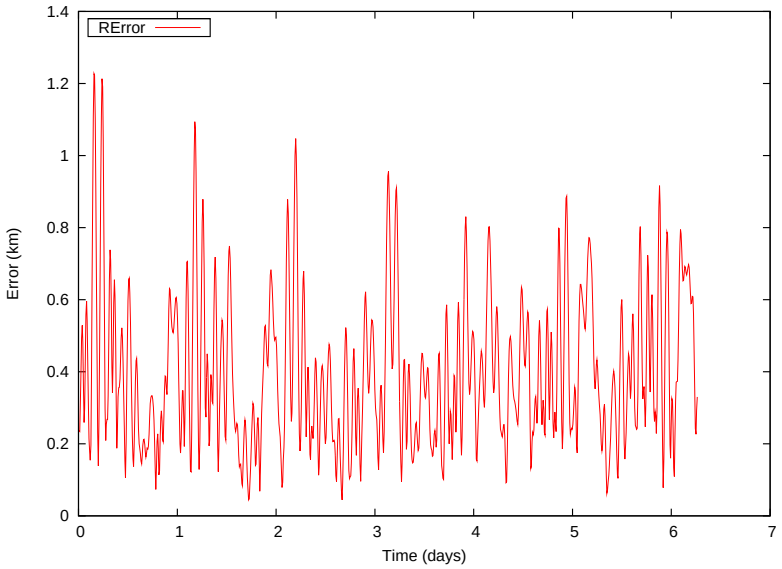

Figure 4.2: SGP4 verification showing residual magnitude for test case.

4.1.2 Reference Satellite. With the SGP4 program working properly, the reference satellite was run next for a fifty-five day period. Figure 4.3 shows individual coordinate residuals as high as six kilometers and Figure 4.4 shows error magnitude at a maximum of seven kilometers during the 55 day period. These plots will be used for comparison later in the paper.

4.2 Comparing SGP4 and STK Propagators

The results of comparing the SGP4 and STK propagators are discussed here. The Grace 1 and Grace 2 satellites were chosen for their similar orbits. Results for these two

Table 4.1: SGP4/STK Satellite Residual Results

Satellite	Comparison Length (days)	Coordinate Residuals			Residual Magnitude (km)
		x (km)	y (km)	z (km)	
Grace 1	25	3.5	4	3	4.5
Grace2	20	3	3.5	2.5	4
SWIFT	25	2	2	3	3
Reference Satellite	55	3	2	3	3.5

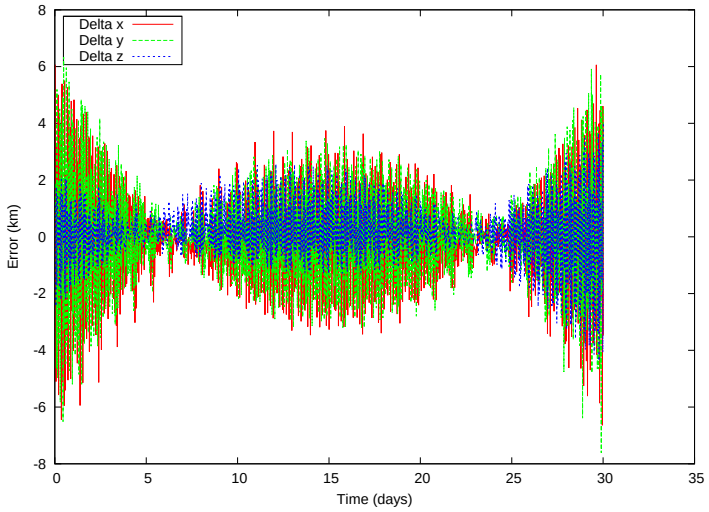

Figure 4.3: SGP4 verification showing coordinate residuals for reference satellite.

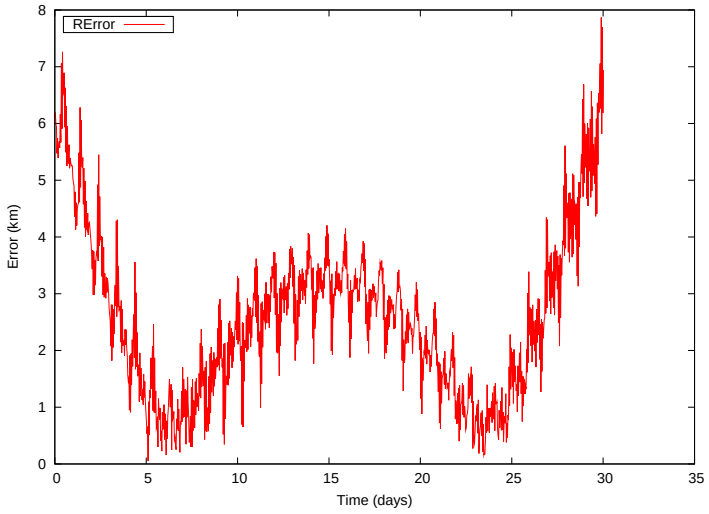

Figure 4.4: SGP4 verification showing residual magnitude for reference satellite.

satellites should be very similar. As can be seen in Figures 4.5 to 4.8, the results are indeed very similar and help to show the program is working correctly. If results for these two satellites had been off, the author would have been alerted to look for an error that otherwise may have gone unnoticed if all satellites were dissimilar.

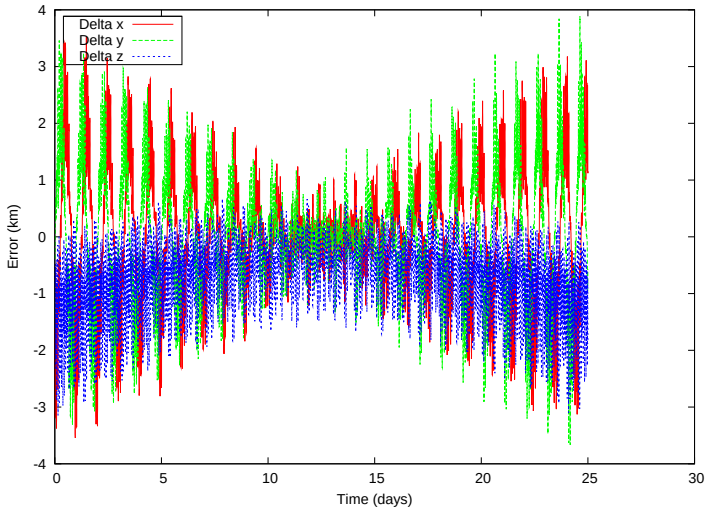

Figure 4.5: SGP4/STK coordinate residuals for Grace 1 satellite.

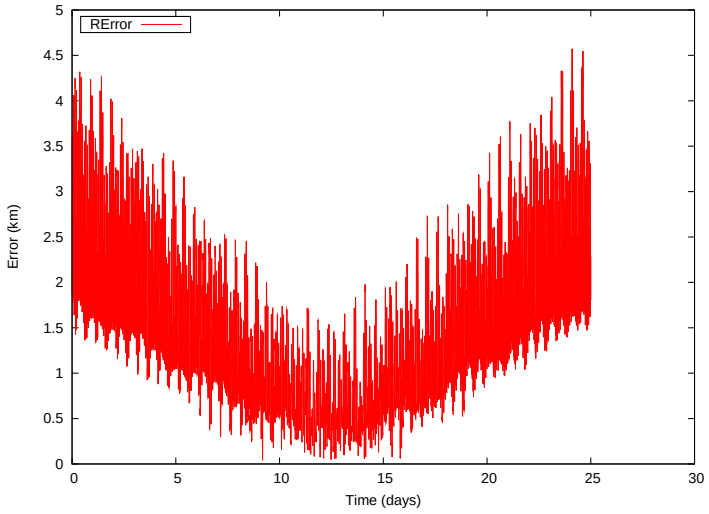

Figure 4.6: SGP4/STK residual magnitude for Grace 1 satellite.

The comparison between SGP4 and STK for the Grace 1 and Grace 2 satellites was good to under 4.5 and 4 kilometers in magnitude respectively. A complete listing of coordinate residuals and residual magnitudes can be seen in Table 4.1 and plots for the remaining satellites can be found in Appendix D.

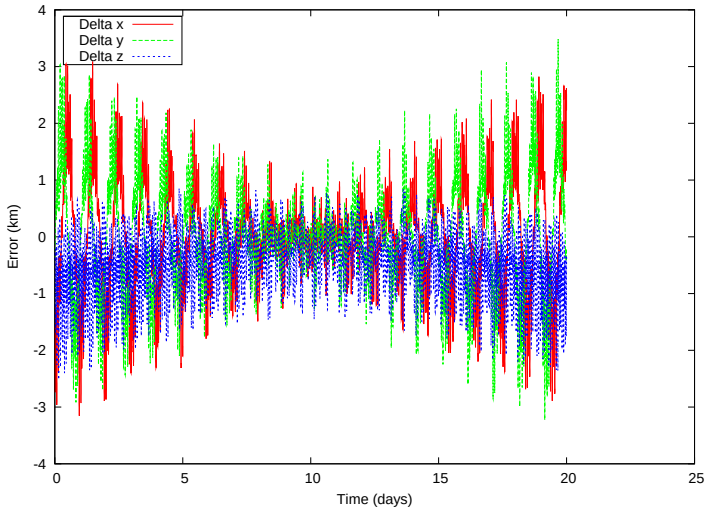

Figure 4.7: SGP4/STK coordinate residuals for Grace 2 satellite.

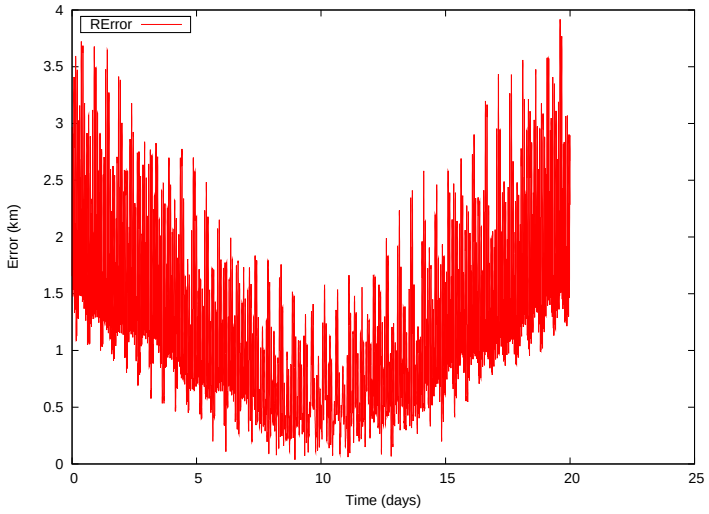

Figure 4.8: SGP4/STK residual magnitude for Grace 2 satellite.

Some satellites tested would not produce residuals under 100 kilometers within the first ten to fifteen days. The actual reason is not know at this time, however there are some possibilities. The original 1980 SGP4 code did have some errors for certain satellite orbits. This was one of the reasons users started modifying the 1980 version. Another possibility is the chance of errors within the least squares converging process.

The matrices can be singular or near singular, with high condition numbers, which could cause problems in convergence.

4.3 STK and Torus Comparison for Reference Satellite

As mentioned earlier. the reference satellite was numerically integrated by Dr. Wiesel for one year. This one year long numerical integration was used to identify the three torus frequencies which describe the reference satellite as a torus in phase space. The reference satellite was propagated for 60 days with STK. This 60 days of orbit data was then fit to the year long reference torus. The differences in individual coordinates and total magnitude were calculated as before and used for plotting.

Initial residuals reached 500 kilometers within 60 days at a linear rate as seen in Figure 4.9.

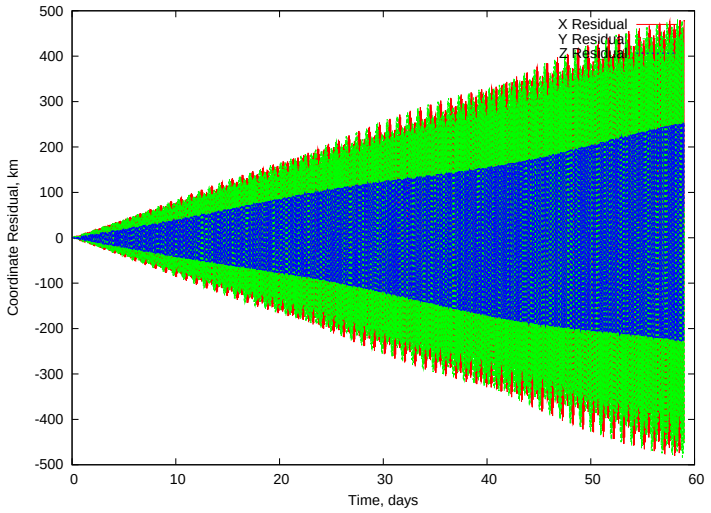

Figure 4.9: Torus vs. STK data coordinate residuals for reference satellite.

Dr. Wiesel suggested the frequencies describing the numerically integrated orbit may differ from the STK orbit frequencies since their calculation methods are different. If the frequencies used to fit the STK orbit data to the reference satellite torus were adjusted, better accuracy could be achieved. Of the three torus frequencies, ω_1, the mean motion, is the largest and would be the one to adjust. First, the slope with which

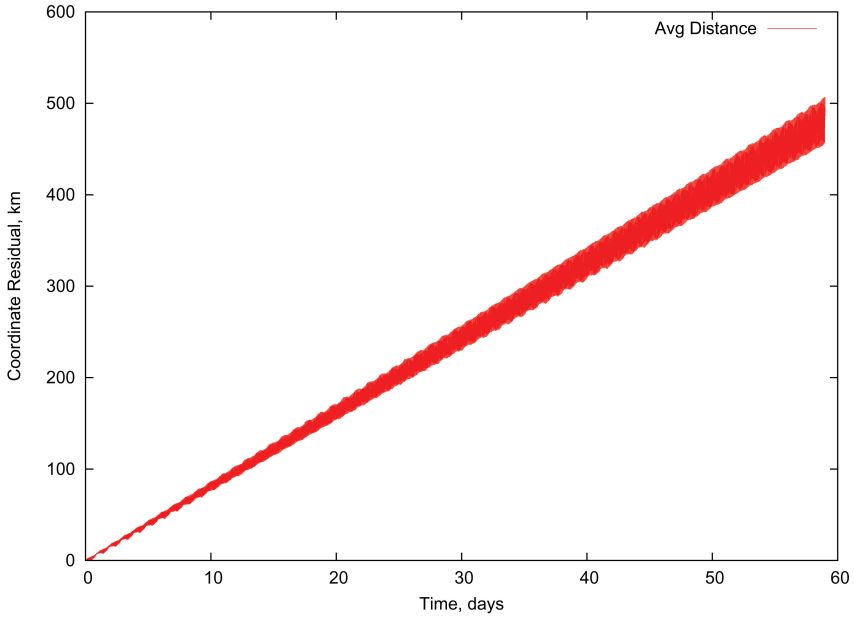

Figure 4.10: Torus vs. STK data residual magnitude for reference satellite.

the residual magnitude rose in Figure 4.10 was found at multiple points and had units of kilometers per day. This was done to get an average value for the entire plot. Each calculated slope was then divided by the distance the point used was from the origin of the ECEF system. This then gave the amount of radians per day the residuals were increasing. Finally, days were converted to time units which are used within the program. The change in frequency was rather small at a 0.0012% change. The average value for the plot was the frequency difference between the numerically integrated torus and the STK orbit data torus. By trial and error it was determined if this value should be added or subtracted from the original torus frequency, ω_1.

After implementing the frequency change and re-running the programs, residuals improved to thirty kilometers within sixty days, or an over 90% improvement. The entire process was completed a second time with the frequency only changing by 6 X 10-5%. However, the residuals again improved to under 5 kilometers in a 60 day period which was another improvement of 80%. These results can be seen in Figures 4.11 to 4.12.

Finally, STK orbit data for the reference satellite was propagated 120 days and fit to the reference satellite torus. As seen in the following plots, coordinate residuals were under three kilometers and residual magnitude remained under 3.5 kilometers.

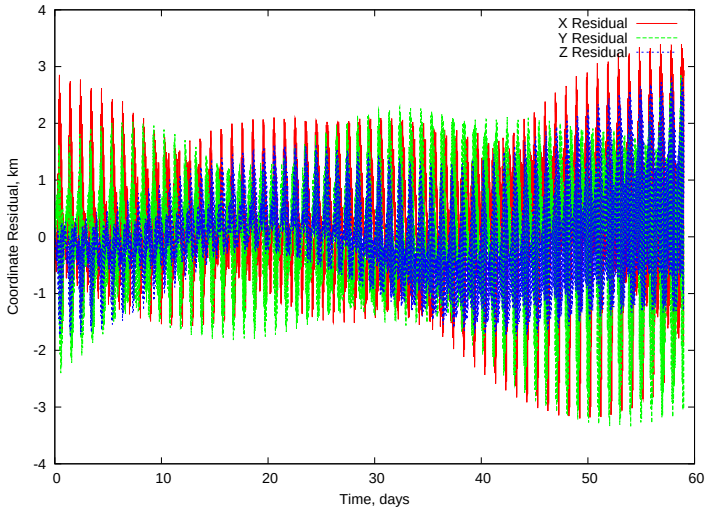

Figure 4.11: Torus vs. STK data coordinate residuals for reference satellite.

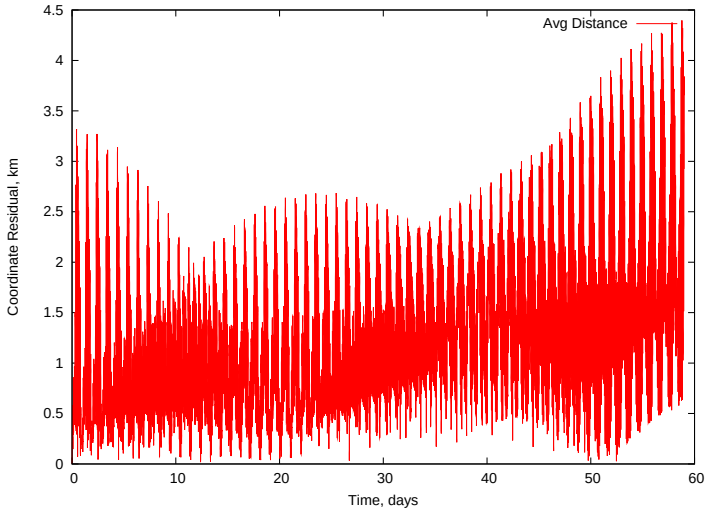

Figure 4.12: Torus vs. STK data residual magnitude for reference satellite.

Recalling Section 4.2, SGP4 was able to compare to STK orbit data for the reference satellite out to 55 days with 3.5 kilometers of residual magnitude error, but could not converge on anything greater than sixty days. The torus model allows much great comparison time periods with equal or better accuracy.

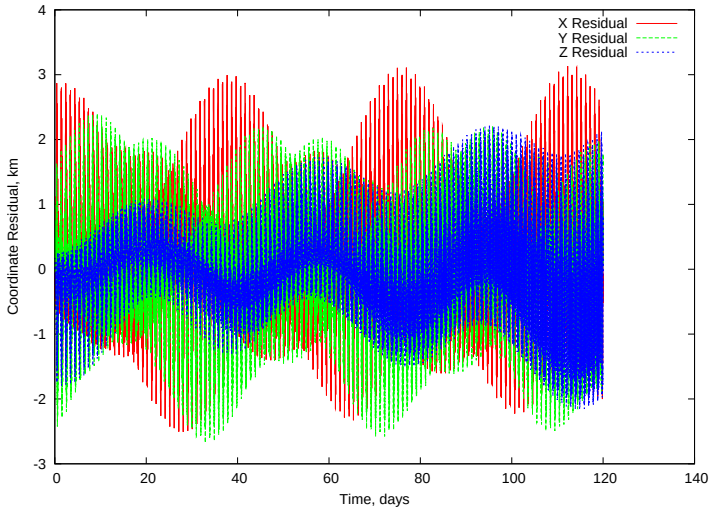

Figure 4.13: Torus vs. STK data coordinate residuals for reference satellite.

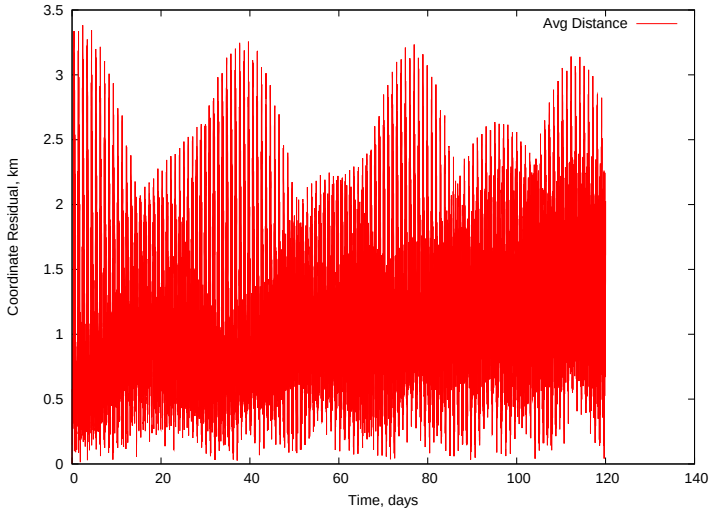

Figure 4.14: Torus vs. STK data residual magnitude for reference satellite.

It is also important to note that when working in the 'fixed' frame in STK, this paper's ECEF frame, some perturbations not included in this paper have been added back in automatically. STK is not intended to be used as a simplified model, so some perturbations were 'hard-coded' into STK. These 'hard-coded' perturbations could be accounting for the patterns seen in the figures presented in this chapter.

V. Conclusions

5.1 Comparing SGP4 and STK

The results from comparing actual satellites with SGP4 and STK propagation methods produce relatively low residuals. In normal location monitoring, times between tracks would probably not reach twenty to twenty-five days as seen here. Therefore the three to five kilometers in magnitude error would be plenty low enough to ensure that satellite was not lost. These results also show how quickly predicted results can become large and how frequently these predictions must be updated to ensure satellite location is known within a reasonable distance and reliability. Applying these techniques to a 17,000 object, and growing, space catalog is indeed a very daunting task.

5.2 KAM Torus Orbit Prediction

The results obtained from comparing STK orbit data with a known KAM torus model were surprisingly accurate. At time periods out to 120 days, individual coordinate residuals remained under three kilometers. Time periods greater than 120 days were tried and could have been presented here. However, at those time lengths STK orbit reliability has diminished with the simplified model being used in this research and any results would not have as much meaning as the more accurate 120 day orbit periods.

With SGP4 and STK orbit prediction techniques, errors slowly start to creep into results and grow as orbit propagation time periods increase. However, the KAM torus model showed constant coordinate residuals. This shows the periodic nature of the KAM torus and the linear drift of the position of the satellite on the torus in phase space keeping the residuals at constant low values. It also shows the theory behind this KAM torus, that lightly perturbed Hamiltonian system's solutions lie on a KAM torus and once on this invariant torus the solution stays on it.

5.3 Recommendations

As part of the initial studies, this research has done very well. The KAM torus model takes into account the entire geopotential model while other existing techniques must estimate the geopotential. However, the KAM torus method does not yet include

other perturbing forces that are commonly accounted for in orbit prediction. A future step would be to incorporate effects such as air drag, lunar effects , and solar effects and verify if the solution to the Hamiltonian still lies on the surface of a torus.

It is believed Dr. Wiesel will be looking into satellites drifting from one invariant torus to a nearby invariant torus, so this topic holds avenues for possible research.

Finally, it would be outstanding to work with an existing satellite team whose satellite has been accurately modeled with current KAM torus methods and work towards updating the KAM torus method to the degree that the satellite team would navigate their satellite with the KAM torus method.

Also, Dr. Wiesel has discussed using KAM torus methods to navigate a constellation of satellites. With the linear drift of a satellite on the surface of a torus in phase space, station keeping between satellites would merely entail maintaining equal linear spacing on the surface of the torus in phase space.

Although KAM theory is relatively old, KAM torus orbit prediction methods are relatively new and hold enormous possibilities for the future. Hopefully these ideas are getting more people interested and the rate of research and testing can increase.

Appendix A. Hamiltonian Mechanics Example

In this appendix, the simple pendulum will be used as an example to illustrate the application of Lagrangian and Hamiltonian mechanics discussed in Chapter II. A simple pendulum is fixed to an upper, non-moving surface. The pendulum is allowed to move sideways in the plane of the paper about the point where it meets the surface.

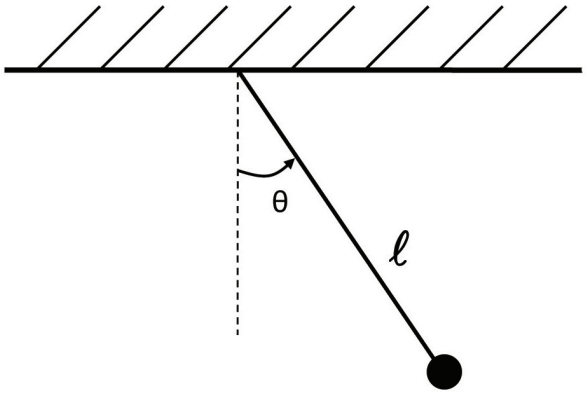

Figure A.1: A Simple Pendulum

As discussed earlier, multiple coordinate systems can usually be used for a given problem. For this problem Cartesian coordinates can be used, but polar coordinates simplify the problem,

$$\boldsymbol{q} = \left\{ \begin{array}{c} l \\ \theta \end{array} \right\}. \tag{A.1}$$

The kinetic energy of the pendulum is,

$$T = \frac{1}{2}mv^2, \tag{A.2}$$

where the velocity for the pendulum is the angular velocity, $v = l\dot{\theta}$. This results in the kinetic energy being,

$$T = \frac{1}{2}ml^2\dot{\theta}^2. \tag{A.3}$$

The potential energy of the pendulum based on its height is,

$$V = mgh. \tag{A.4}$$

The height of the pendulum mass can be determined from its vertical distance, $h = -l\cos\theta$, which gives a potential energy of,

$$V = mg(-l\cos\theta) = -mgl\cos\theta. \tag{A.5}$$

As mentioned in Section 2.1.3, the Lagrangian of a system is the kinetic energy minus the potential energy, and for this system is,

$$\pounds = T - V = \frac{1}{2}ml^2\dot{\theta}^2 - (-mgl\cos\theta) = \frac{1}{2}ml^2\dot{\theta}^2 + mgl\cos\theta. \tag{A.6}$$

To simplify the problem, the Lagrangian per unit mass will be used instead,

$$\pounds = \frac{\pounds}{m} = \frac{1}{2}l^2\dot{\theta}^2 + gl\cos\theta. \tag{A.7}$$

Remembering the generalized velocities are,

$$\dot{\boldsymbol{q}} = \begin{Bmatrix} \dot{l} \\ \dot{\theta} \end{Bmatrix}, \tag{A.8}$$

and the Lagrangian equations of motion (EOM) come from,

$$\frac{d}{dt}\left(\frac{\partial\pounds}{\partial\dot{q}_k}\right) - \frac{\partial\pounds}{\partial q_k} = 0, \tag{A.9}$$

the Lagrangian equations of motion (EOM) can be solved for,

$$l^2\ddot{\theta} + gl\sin\theta = 0. \tag{A.10}$$

However, in this example the Hamiltonian is being solved. The generalized momenta is,

$$p_\theta = \frac{\partial\pounds}{\partial\dot{\theta}} = l^2\dot{\theta}. \tag{A.11}$$

The Hamiltonian comes from,

$$\mathcal{H} = \sum_{k=1}^{n} p_k \dot{q_k} - \pounds. \tag{A.12}$$

Solving for the generalized velocity from the generalized momenta,

$$\dot{\theta} = \frac{p_\theta}{l^2}, \tag{A.13}$$

and substituting into the Hamiltonian gives,

$$\mathcal{H} = \frac{1}{2}\frac{{p_\theta}^2}{l^2} - gl\cos\theta). \tag{A.14}$$

The Hamilton canonical equations come from,

$$\dot{q_k} = \frac{\partial \mathcal{H}}{\partial p_k}, \tag{A.15}$$

$$\dot{p_k} = -\frac{\partial \mathcal{H}}{\partial q_k}, \tag{A.16}$$

and are,

$$\dot{\theta} = \frac{p_\theta}{l^2}, \tag{A.17}$$

$$\dot{p_\theta} = -gl\sin\theta. \tag{A.18}$$

Appendix B. Earth Orbiting Satellite Hamiltonian Derivation

In this appendix, the Hamiltonian for the Earth orbiting reference satellite used throughout this paper will be derived. The same steps seen in the simple pendulum example in Appendix A will be followed.

For the Earth orbiting satellite problem, an Earth-Centered, Earth-Fixed (ECEF) frame of reference will be used. Regular Cartesian coordinates (x, y, z) will be used to describe position,

$$\boldsymbol{q} = \left\{ \begin{array}{c} x \\ y \\ z \end{array} \right\}. \tag{B.1}$$

The velocity of the satellite is simply the time derivative of the position. However, remember the ECEF reference frame is rotating, so to get the true velocity an additional term must be added to take into account this rotation about the z-axis.

$$\dot{\boldsymbol{q}} = \left\{ \begin{array}{c} \dot{x} - \omega_{\oplus} y \\ \dot{y} + \omega_{\oplus} x \\ \dot{z} \end{array} \right\} \tag{B.2}$$

The kinetic energy can then be determined by simply plugging the velocity into Equation 2.4,

$$T = \frac{1}{2} m((\dot{x} - \omega_{\oplus} y)^2 + (\dot{y} + \omega_{\oplus} x)^2 + \dot{z}^2). \tag{B.3}$$

For simplicity, it is not uncommon to divide the above equation through by the mass which then gives kinetic energy per unit mass. One reason for doing this is not being required to carry the mass throughout then entire process that follows, while another is the mass may not yet me know for the satellite. Either way, in this paper the kinetic energy and all quantities with mass that follow will be per unit mass.

$$T = \frac{1}{2}((\dot{x} - \omega_{\oplus} y)^2 + (\dot{y} + \omega_{\oplus} x)^2 + \dot{z}^2). \tag{B.4}$$

The potential energy, as discussed in Section 2.2.1, is given by,

$$V = -\frac{\mu}{r}\sum_{n=1}^{\infty}\sum_{m=1}^{n}(\frac{r}{R_\oplus})^{-n}P_n^m(\sin\delta)(C_{nm}\cos m\lambda + S_{nm}\sin m\lambda). \tag{B.5}$$

The Lagrangian is then found by plugging the kinetic and potential energy into equation B.6,

$$\pounds = \frac{1}{2}((\dot{x}-\omega_\oplus y)^2+(\dot{y}+\omega_\oplus x)^2+\dot{z}^2)-\frac{\mu}{r}\sum_{n=1}^{\infty}\sum_{m=1}^{n}(\frac{r}{R_\oplus})^{-n}P_n^m(\sin\delta)(C_{nm}\cos m\lambda+S_{nm}\sin m\lambda). \tag{B.6}$$

The canonical momenta are obtained using equation 2.8,

$$\boldsymbol{p} = \left\{\begin{array}{c} p_x \\ p_y \\ p_z \end{array}\right\} = \left\{\begin{array}{c} \dot{x}-\omega_\oplus y \\ \dot{y}+\omega_\oplus x \\ \dot{z} \end{array}\right\}. \tag{B.7}$$

Finally, the Hamiltonian is obtained using equation 2.10,

$$\begin{aligned}\mathcal{H} = \frac{1}{2}(p_x^2+p_y^2+p_z)^2 + \omega_\oplus(yp_x - xp_y) \\ -\frac{\mu}{r}\sum_{n=1}^{\infty}\sum_{m=1}^{n}(\frac{r}{\Re})^{-n}P_n^m(\sin\delta)(C_{nm}\cos m\lambda + S_{nm}\sin m\lambda)\end{aligned} \tag{B.8}$$

Appendix C. Non-linear Least Squares Estimation within SGP4

C.1 Least Squares Origin

The least squares estimation process is a method of using observations, or data points, to accurately predict the next data point for a system. Consider a non-linear system for which the solution is a function of time,

$$\boldsymbol{x}(t) = \boldsymbol{h}(\boldsymbol{x}(t_0), t). \tag{C.1}$$

If the initial location and time are know, the current location can be found. In this paper, the above system is the orbiting satellite being propagated via SGP4.

The data the author would like SGP4 to model is the STK orbit data which will be called the observations, $\boldsymbol{z}$. For each step through time, SGP4 results will be compared to the STK data. The difference between the two is an error, since the ideal case would be for SGP4 to exactly match STK and produce no error. The error is the SGP4 location minus the STK location for each time step,

$$\boldsymbol{e} = \boldsymbol{x} - \boldsymbol{z}. \tag{C.2}$$

These errors are then added up to determine the total error produced during the propagation,

$$E = \sum_{i=1}^{N} e_i. \tag{C.3}$$

The case in which SGP4 propagation best matched the STK data should create the smallest total error, E. However, if the SGP4 data was smaller than the STK data for a given time step a negative number would be produced. When added up at the end, this would make the total error look smaller even though it was not. To fix this problem the individual errors for each time step are squared, ensuring all numbers are positive,

$$\boldsymbol{e}^2 = (\boldsymbol{x} - \boldsymbol{z})^2. \tag{C.4}$$

These squared errors are then added up at the end to produce a total squared error,

$$E^2 = \sum_{i=1}^{N} e_i^2. \tag{C.5}$$

Even though the errors have been squared, the case in which SGP4 and STK matched the best would still be when the squared error was the least. This is where least squares estimation gets its name.

C.2 Non-Linear Least Squares

Starting with Equation C.1, SGP4 will propagate a satellite through time non-linearly. As mentioned earlier, this is completed by incrementing the orbital elements through time to produce a new location and velocity. The *state* of the satellite will be used to refer to its position and velocity,

$$\boldsymbol{x} = \left\{ \begin{array}{c} x \\ y \\ z \\ \dot{x} \\ \dot{y} \\ \dot{z} \end{array} \right\}. \tag{C.6}$$

In an effort to predict the future state of the system, the dynamics (Equation C.1) will be linearized. Essentially, to get from the starting point to the ending point a bunch of small steps will be taken. To get from one state to the next state, a state transition matrix, $\boldsymbol{\Phi}$, is use,

$$\delta\boldsymbol{x}(t_{i+1}) = \boldsymbol{\Phi}(t_{i+1}, t_i)\delta\boldsymbol{x}(t_i), \tag{C.7}$$

where the next state is,

$$\boldsymbol{x}(t_{i+1}) = \boldsymbol{x}_i + \delta\boldsymbol{x}(t_{i+1}), \tag{C.8}$$

Earlier it was said the SGP4 process is non-linear. The entire SGP4 process will be represented by a non-linear function, $\boldsymbol{G}$, such that the state (Equation C.6) and time

put through this function will produce the correct STK orbit data ($\boldsymbol{z}$) for that time,

$$\boldsymbol{z}_i(t_i) = \boldsymbol{G}(\boldsymbol{x}(t_i), t_i). \tag{C.9}$$

Equation C.9 will be called the observation relation. Although the STK orbit data is considered the truth model, there is still error within it. The assumptions made within the STK program create errors that make the STK state of the satellite differ from the actual state of the satellite. The difference between the STK state and true state can be represented as an error,

$$\boldsymbol{e} = \boldsymbol{z} - \boldsymbol{z}_0. \tag{C.10}$$

Applying Equation C.9 to Equation C.10, and then substituting in Equation C.8 produces,

$$\boldsymbol{e} = \boldsymbol{G}(\boldsymbol{x}, t) - \boldsymbol{G}(\boldsymbol{x}_0, t) = \boldsymbol{G}(\boldsymbol{x}_0 + \delta\boldsymbol{x}, t) - \boldsymbol{G}(\boldsymbol{x}_0, t). \tag{C.11}$$

After expanding and subtracting,

$$\boldsymbol{e} \approx \frac{\partial \boldsymbol{G}}{\partial \boldsymbol{x}} \delta\boldsymbol{x}(t). \tag{C.12}$$

This represents the true error in the STK orbit data. It is assumed this true error in the data will equal the residual in the data, $\boldsymbol{e} \approx \boldsymbol{r}$. The partial fraction matrix in Equation C.12 relates the error in the state to the error in the reference trajectory,

$$H_i(t_i) = \frac{\boldsymbol{G}}{\boldsymbol{x}}(\boldsymbol{x}_{ref}(t_i), t_i). \tag{C.13}$$

The residual can then be calculated on the reference trajectory,

$$\boldsymbol{r}_i = \boldsymbol{z}_i - \boldsymbol{G}(\boldsymbol{x}_{ref}(t_i), t_i). \tag{C.14}$$

Remembering Equation C.7 and applying it to Equation C.14 produces,

$$\boldsymbol{r}_i \approx H_i \delta\boldsymbol{x}(t_i) = H_i \Phi(t_i, t_0) \delta\boldsymbol{x}(t_0), \tag{C.15}$$

$$\boldsymbol{r} = T_i \delta \boldsymbol{x}(t_0), \tag{C.16}$$

where $T = H\Phi$. From this relation, once the residuals, r, are determined the correction, $\delta \boldsymbol{x}(t_0)$, can be found. However, the T matrix cannot simply be divided through like a scalar value. Its inverse may also not be able to be determined, so another method must be used. First, the transpose of T is left multiplied to each side of Equation C.16.

$$T^T \boldsymbol{r} = T^T T \delta \boldsymbol{x}(t_0). \tag{C.17}$$

The operation $T^T T$ is guaranteed to produce a square matrix which the inverse can then be taken to solve for $\delta \boldsymbol{x}(t_0)$,

$$\delta \boldsymbol{x}_0 = (T^T T)^{-1} T^T \boldsymbol{r}. \tag{C.18}$$

This change added to the initial trajectory produces a better trajectory,

$$\boldsymbol{x}_0 = \boldsymbol{r}_{ref}(t_0) + \delta \boldsymbol{x}_0. \tag{C.19}$$

This process is continued until the change is less than a tolerance or a certain number of iterations is reached.

D.1 SGP4/STK Residual Plots

In this appendix, all plots from the discussion in Section 4.2 concerning the comparison of the SGP4 and STK propagators will be shown. As a reminder, coordinate residual plots show the difference between the individual coordinates (x, y, z) in the two propagators. Residual magnitude plots show the magnitude of all the coordinate residuals.

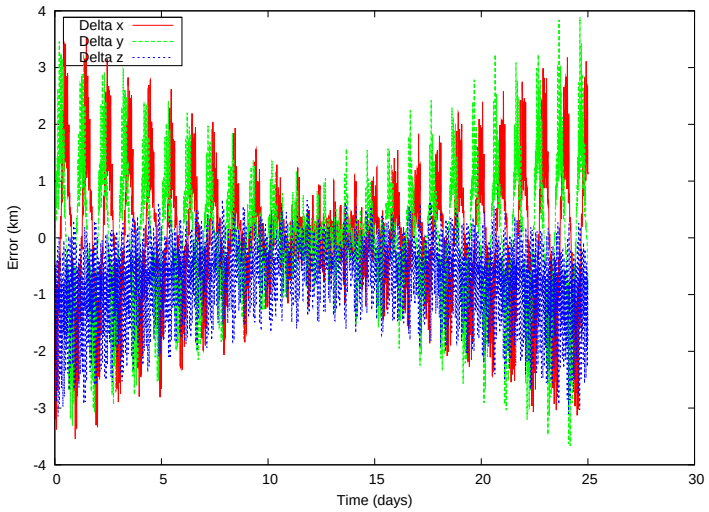

(a)

Figure D.1: SGP4/STK coordinate residuals for Grace 1 satellite.

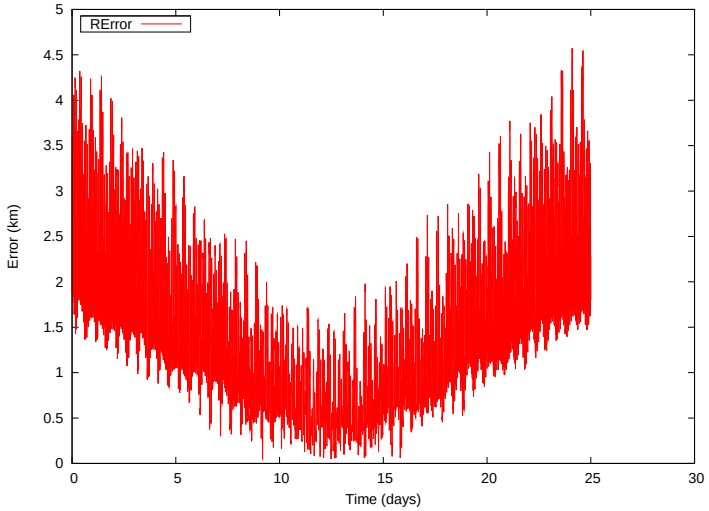

(a)

Figure D.2: SGP4/STK residual magnitude for Grace 1 satellite.

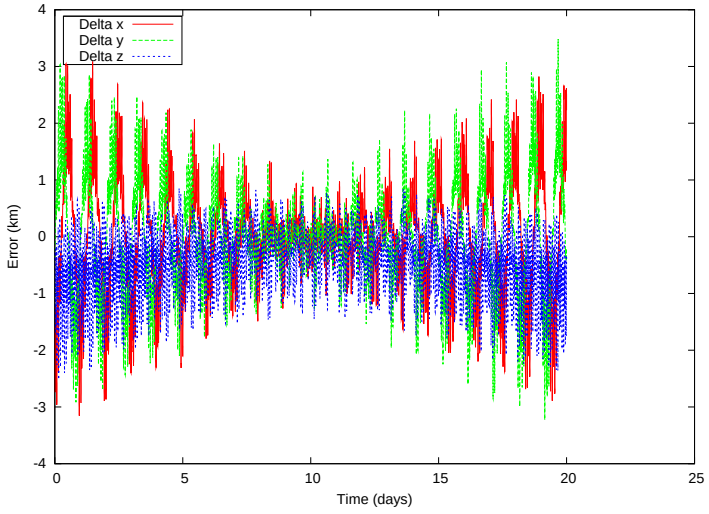

(a)

Figure D.3: SGP4/STK coordinate residuals for Grace 2 satellite.

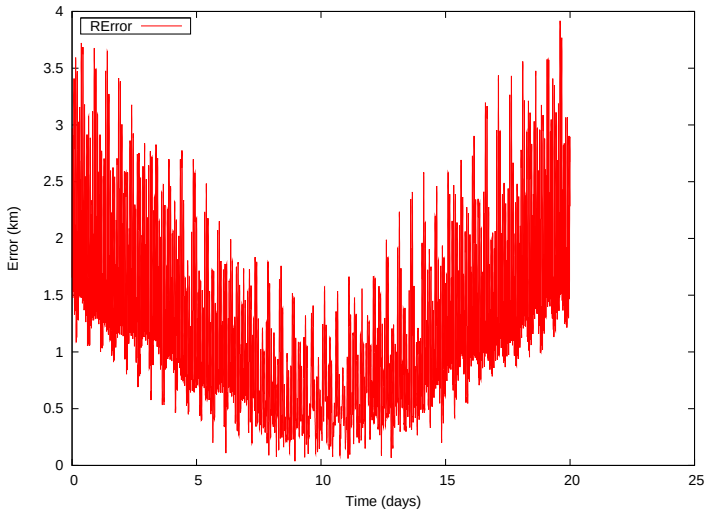

(a)

Figure D.4: SGP4/STK residual magnitude for Grace 2 satellite.

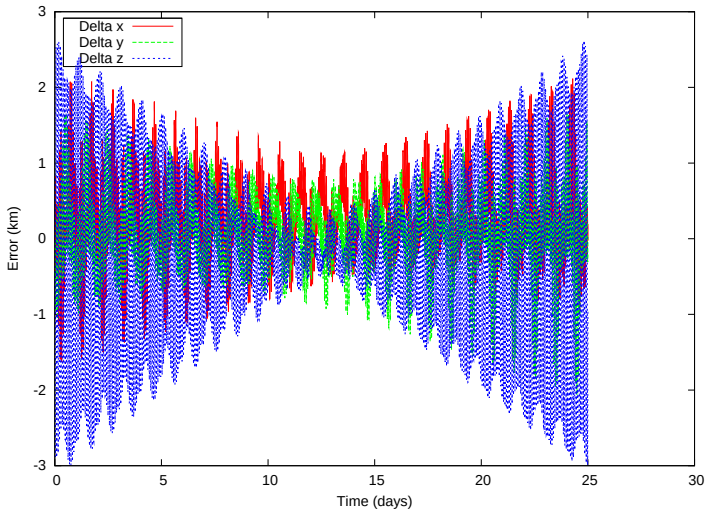

(a)

Figure D.5: SGP4/STK coordinate residuals for SWIFT satellite.

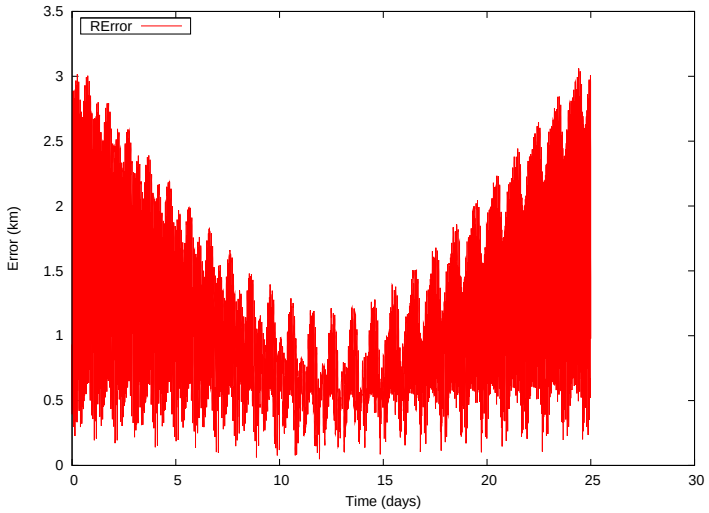

(a)

Figure D.6: SGP4/STK residual magnitude for SWIFT satellite.

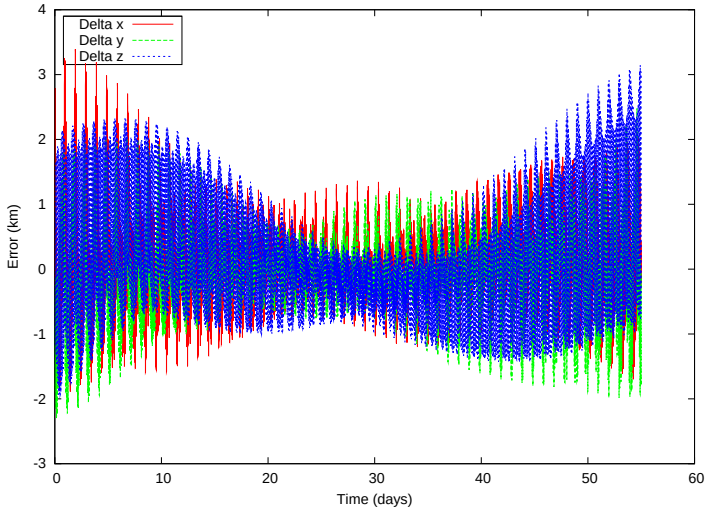

(a)

Figure D.7: SGP4/STK coordinate residuals for Reference Satellite.

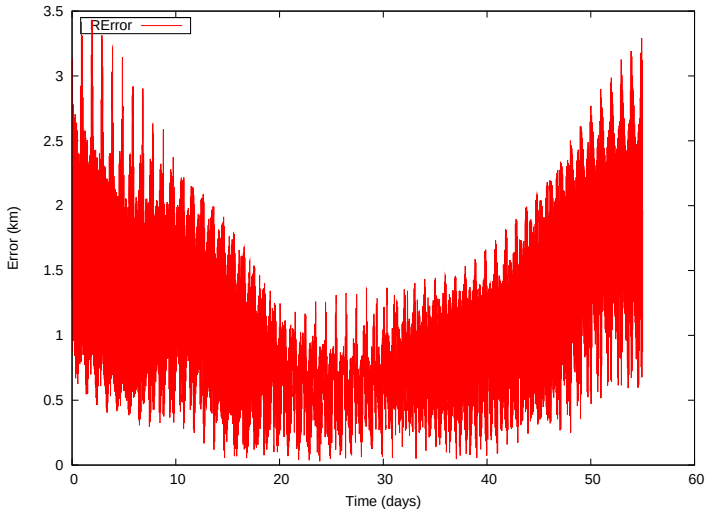

(a)

Figure D.8: SGP4/STK residual magnitude for Reference Satellite.

Bibliography

1. "Illustration of geographic and geocentric latitudes," `http://en.wikipedia.org/wiki/File:Two-types-of-latitude.png`, 2008.
2. "GRACE Gravity Model 01 Europe and Africa," `http://www.csr.utexas.edu/grace/gallery/gravity/ggm01_euro2.html`, 2004.
3. "USSTRATCOM Space Control and Space Surveillance Fact Sheet," 2010.
4. National Aeronautics and Space Administration, Wahington, DC, *NASA-HANDBOOK 8719.14*, 2008.
5. Howe, Adele; Whitley, L. D., "Advanced Air Force Scheduling through Modeling Problem Topologies," Tech. Rep. F49620-03-1-0233, Computer Science Department, Colorado State Univeristy, August 2006.
6. Olivier, Scot, Cook, Kem, and Fasenfest, David, "High-Performance Computer Modeling of the Cosmos-Iridium Collision," No. LLNL-CONF-416345, Lawrence Livermore National Laboratory, Advanced Maui Optical and Space Surveillance Conference, Livermore, CA, 2009.
7. Wiesel, W. E., "Earth Satellite Orbits as KAM Tori," *The Journal of the Astronautical Sciences*, Vol. 56, No. 2, 2008, pp. 151–162.
8. Little, B. D., *Earth Satellite Orbits as KAM Tori*, Master's thesis, Air Force Institute of Technology, March 2009.
9. Pars, L. A., *A Treatise On Analytical Dynamics*, Ox Bow Press, Woodbridge, CT, 1979.
10. Meirovitch, L., *Methods of Analytical Dynamics*, Dover Publications, Inc., Mineola, New York, 1998.
11. Vallado, David A., Crawford, Paul, Hujsak, Richard, and Kelso, T.S., "Revisiting Spacetrack Report #3," *American Institute of Aeronautics and Astronautics*, , No. AIAA 2006-6753, 2006.
12. Hoots, Felix R and Roehrich, Ronald L., "Spacetrack Report No. 3," December 1988.
13. Wiesel, W. E., *Modern Astrodynamics*, Aphelion Press, Beavercreek, OH, 2003.
14. Nakane, Michiyo and Fraser, Craig G., "The Early History of Hamilton-Jacobi Dynamics 1834-1837," *Centaurus*, Vol. 44, 2002, pp. 161–227.
15. Wiesel, W. E., "Motion Near A KAM Torus," Awaiting publishing.
16. Wiesel, W. E., "Earth Satellite Perturbation Theories As Approximate KAM Tori," Awaiting publishing.
17. Arnold, V., *Mathematical Methods of Classical Mechanics*, Springer Science+Business Media, LLC, New York, New York, 1989.

REPORT DOCUMENTATION PAGE

Form Approved
OMB No. 0704–0188

1. REPORT DATE (DD–MM–YYYY)	2. REPORT TYPE	3. DATES COVERED *(From — To)*
25-03-2010	Master's Thesis	May 2008 – March 2010

4. TITLE AND SUBTITLE
Verification of KAM Theory on Earth Orbiting Satellites

5a. CONTRACT NUMBER

5b. GRANT NUMBER

5c. PROGRAM ELEMENT NUMBER

6. AUTHOR(S)
LT CHRISTIAN BISHER

5d. PROJECT NUMBER

5e. TASK NUMBER

5f. WORK UNIT NUMBER

7. PERFORMING ORGANIZATION NAME(S) AND ADDRESS(ES)
Air Force Institute of Technology
Graduate School of Engineering and Management (AFIT/ENY)
2950 Hobson Way
WPAFB OH 45433-7765

8. PERFORMING ORGANIZATION REPORT NUMBER
AFIT/GAE/ENY/10-M03

9. SPONSORING / MONITORING AGENCY NAME(S) AND ADDRESS(ES)

Intentionally left blank

10. SPONSOR/MONITOR'S ACRONYM(S)

11. SPONSOR/MONITOR'S REPORT NUMBER(S)

12. DISTRIBUTION / AVAILABILITY STATEMENT
APPROVED FOR PUBLIC RELEASE; DISTRIBUTION UNLIMITED

13. SUPPLEMENTARY NOTES

14. ABSTRACT

This paper uses KAM torus theory and Simplified General Perturbations 4 (SGP4) orbit prediction techniques compiled by Dr. William Wiesel and compares it to Analytical Graphics® Incorporated (AGI) Satellite Toolkit® (STK) orbit data. The goal of this paper is to verify KAM torus theory can be used to describe and propagate an Earth satellite orbit with similar accuracy to existing general perturbation techniques. Using SGP4 code including only truncated geopotential effects, KAM torus generating code, and other utilities were used to describe a particular satellite orbit as a torus and then propagate the satellite using traditional and KAM torus techniques. These results were compared with similar data generated from initial conditions in STK. Comparisons show orbit prediction for this particular satellite can be made with low kilometer level accuracy. It is claimed with increased mathematical precision and orbital model detail, KAM torus theory applied to orbit prediction techniques can produce more accurate results than currently achievable.

15. SUBJECT TERMS
KAM Theory, Earth Satellites, Hamiltonian

16. SECURITY CLASSIFICATION OF: UNCLASSIFIED			17. LIMITATION OF ABSTRACT	18. NUMBER OF PAGES	19a. NAME OF RESPONSIBLE PERSON
a. REPORT	b. ABSTRACT	c. THIS PAGE	UU	64	William E. Wiesel Jr., PhD (ENY)
U	U	U			19b. TELEPHONE NUMBER (Include Area Code) (937)255-3636, ext 4312